

Qubit-qudit entanglement transfer in defect centers with high-spin nuclei

Wolf-Rüdiger Hannes and Guido Burkard

Department of Physics and IQST, University of Konstanz, 78457 Konstanz, Germany

We propose a scheme for accumulating entanglement between long-lived qudits provided by central nuclear spins of defect centers. Assuming a generic setting, the electron spin of each node acts as the communication qubit and may be entangled with other nodes, e.g., through a spin-photon interface. The generally available Ising component of the hyperfine interaction is shown to facilitate repeated entanglement transfer onto memory qudits of arbitrary dimension $d \leq 2I + 1$ with I the nuclear spin quantum number. When d is set to an integer power of two, maximal entanglement can be generated deterministically and without intermittent driving of nuclear spins. The scheme is applicable to several candidate systems, including the ^{73}Ge germanium vacancy in diamond.

I. INTRODUCTION

High-spin nuclei in solids comprise a new and rapidly developing platform for quantum information processing (QIP) [1]. In addition to their superior coherence times, such spins offer the advantage of a large Hilbert space, allowing for advanced techniques in various QIP strategies. In the field of quantum error correction, their spin subspace has been identified as a hardware-efficient structure for encoding fault-tolerant logical qubits [2–4]. Advantages over traditional spin qubits could also arise in QIP strategies which do not involve quantum error correction on the lowest level, but instead use the multilevel space directly as a qudit. This includes both the field of quantum communication (QC) [5] and measurement-based quantum computing (MBQC) [6–8]. Several theoretical studies [9–11] have addressed high-dimensional one-way quantum processing, while experimentally, first proof-of-concept operations have been demonstrated [12].

A promising route towards scalable quantum networking is based on devices comprising several modules, where each module consists of an optically addressable defect center in a solid matrix, featuring both an electron and one (or more) nuclear spins, which serve as communication and memory qubits, respectively. In this context, a single network node [13] and a two-node quantum network with remote entanglement storage [14] have recently been realized, both works based on silicon-vacancy centers (SiVs) in diamond-based nanophotonic cavities. At the same time, a higher-dimensional nuclear-spin platform with very similar properties is currently being established [15], namely the ^{73}Ge germanium vacancy (GeV) in diamond with nuclear spin $I = 9/2$. Thus, it is foreseeable that at some point such a quantum network will be extended to high-spin nuclei with the above-mentioned advantages. Another promising type of higher-dimensional nuclear-spin platforms is provided by implanted group V donors in silicon. In this case, the route towards scaling up is somewhat different from the above, and several methods of coupling over microscopic distances have been proposed [16]. However, most of these methods, e.g., the coupling via microwave photons, connect the nuclear spin qudits indirectly via their respective electron spin qubits so that the situation is in principle similar to the optical network device with macroscopically separate nodes.

A natural question for such systems, in particular in view

of higher-dimensional MBQC and QC protocols, is whether a maximally entangled state can be generated between two distant memory qudits, if they only interact with their respective electron spin qubit. Here we provide a solution to this problem considering a hyperfine tensor structure common for central nuclear spins. Generalizing the qubit scheme based on the ^{15}N nitrogen vacancy (NV) center [17] to qudit dimensions $d > 2$, we show that the Ising part may be exploited to realize repeated entanglement transfer, also known as entanglement accumulation [18]. A driving-free and particularly simple version of an iterative scheme results in maximal entanglement deterministically if d is an integer power of two, or with success rate $1/d$ for all other values of d . For specific unfavorable qudit dimensions d , other schemes with higher transfer success rates are constructed. Another option pursued for the unfavorable dimensions d is the generation of highly but partially entangled states, which may still be useful to some extent, even though not allowing perfectly reliable QC protocols [19].

In the case of the ^{15}NV center, driving the nuclear spin is slow due to the small gyromagnetic ratio, but can be enhanced by the hyperfine coupling [17]. For higher spins, while the hyperfine coupling is typically much stronger, such operations could still be relatively slow due to the large number of nearly resonant transitions. Thus we focus on schemes where driving is required only for initialization and, if desired, final state correction; these schemes do not pose any additional demands on the controlling hardware in comparison with the qubit scheme [17]. In the bipartite scenario, our focus is on generating *any* maximally entangled state, and we discuss the explicit form of the state only in special cases.

The model on which our scheme is based is applicable to a wide range of nuclear spins $I \geq 1$ in appropriate parameter regimes. In diamond, aside from the GeV [15] there is also the ^{14}NV center with $I = 1$ which could allow qutrit applications [20]. Considering other host materials, the vanadium ^{51}V defect in silicon carbide [21] with $I = 7/2$ is recently attracting attention. In addition to those defects, whose electron-nuclear spin dynamics is explicitly shown to qualify, several other defects could be potential candidates. One category, already mentioned above, are implanted group-V donors in silicon, in particular ^{75}As with $I = 3/2$ [22], ^{123}Sb with $I = 7/2$ [1, 23, 24], and ^{209}Bi with $I = 9/2$ [25]. Another emerging platform consists of single rare-earth ions,

some of which can be made optically addressable by single photons [26, 27] and strongly couple to (e.g., aluminium nuclear spins with $I = 5/2$ [28]) or host (e.g., ^{141}Pr with $I = 5/2$ [29, 30], ^{143}Nd with $I = 7/2$, or ^{167}Er with $I = 7/2$) high nuclear spins, even though coherent control would have to be demonstrated for some of those examples. While two of these spin quantum numbers ($3/2, 7/2$) just fit a power-of-two dimensional qudit, applying the driving-free scheme to others is possible by lowering d from $2I+1$ to the next favorable number, which can be achieved by leaving the difference number of levels unoccupied during initialization.

The paper is structured as follows. In Sec. II we describe the problem of qubit-qudit entanglement transfer in a general context and derive explicit conditions to be fulfilled in specific iterations. Sec. III contains the model for a single network node and a description of the photonic scheme as an example mechanism for generating internode entanglement links. Using this model, entanglement accumulation schemes are constructed for two nodes in Sec. IV, including both deterministic and probabilistic protocols. The successive application of one selected scheme to pairs of nodes in a larger quantum network is demonstrated to result in higher-dimensional multipartite entanglement in Sec. V. Some further technical aspects are discussed in Sec. VI.

II. BASIC PRINCIPLES

A. Entanglement measure and effective gate

We consider two nodes labeled by the index $K = a, b$, each consisting of an ancillary qubit (states $|0\rangle$ and $|1\rangle$) and a memory qudit of dimension d . While this subsection is model-independent, we refer to the qubit and qudit as electron and nuclear spin, respectively. Prior to the scheme, nuclear spins are initialized in a suitable product state $|\psi^{(0)}\rangle$. One iteration of entanglement transfer consists of three steps: (i) generation of an entangled state (denoted $|\phi_{ee}\rangle$) of the two distant electron spins, (ii) in each node K a controlled gate, denoted $C(U_{K,0}, U_{K,1}) = |0\rangle\langle 0| \otimes U_{K,0} + |1\rangle\langle 1| \otimes U_{K,1}$, between electron and nuclear spins, where $U_{K,0}$ and $U_{K,1}$ commute, and (iii) measurement of both electron spins in the X basis (or along any other axis perpendicular to Z), with outcomes denoted by $j_a, j_b \in \{0, 1\}$. The state into which nuclear spins are projected depends on the measurement outcomes, and its entanglement may generally also depend. We call the process a deterministic complete entanglement transfer if for any measurement outcome, the entanglement is fully transferred. Fig. 1 shows a circuit with $C(U_{K,0}, U_{K,1})$ realized by CPHASE gates, fitting to the model to be considered later.

First, we introduce a method to assess two-qudit entanglement. Consider some bases $\{|u_i\rangle_a\}$ and $\{|u_i\rangle_b\}$ for the two subsystems, where $i = 1, \dots, d$. A general pure two-qudit state is expanded in this basis as $|\psi\rangle = \sum_{i_a, i_b} c_{i_a, i_b} |u_{i_a}\rangle_a \otimes |u_{i_b}\rangle_b$, with the norm $\sum_{i_a, i_b} |c_{i_a, i_b}|^2$. It is convenient to define a $d \times d$ matrix ψ from the coefficients so that the vectorization of ψ^\top gives the state vector $|\psi\rangle$ in this basis. Local operations, $O_a \otimes O_b |\psi\rangle$, are translated as $O_a \psi O_b^\top$. The Schmidt

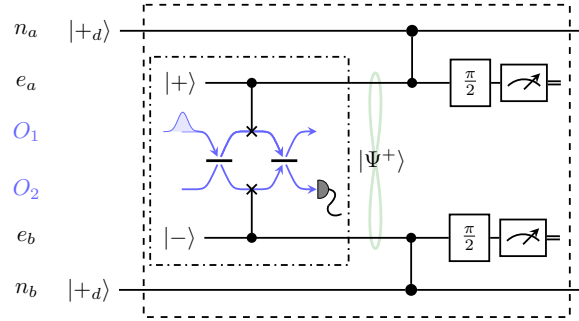


FIG. 1. Scheme for iteratively entangling two memory qudits n_a, n_b . The dash-dotted box contains the photonic setup with optical arms O_1 and O_2 for entangling remote electron spin qubits e_a, e_b , producing the Bell state $|\Psi^+\rangle$. The dashed box corresponds to one iteration of entanglement transfer. The $\frac{\pi}{2}$ -gates are $Y^{1/2}$ rotations. The nuclear initial state $|+d\rangle$ is defined in (26).

decomposition of $|\psi\rangle$ corresponds to the singular value decomposition of ψ , with the singular values or Schmidt coefficients denoted by $\{\sqrt{\chi_k}\}$ and fulfilling $\sum_k \chi_k = 1$. The reduced density matrix $\rho_a = \text{Tr}_b |\psi\rangle\langle\psi|$ is given by $\rho_a = \psi\psi^\dagger$ (and $\rho_b = (\psi^\dagger\psi)^\top$) and its eigenvalues are $\{\chi_k\}$. For pure states, a unique entanglement measure exists, given by the von Neumann entropy of the reduced density matrix (ρ_a or ρ_b), or equivalently the Shannon entropy of the squared Schmidt coefficients,

$$E = -\text{Tr} \rho_a \log_2 \rho_a = -\sum_k \chi_k \log_2 \chi_k. \quad (1)$$

The state $|\psi\rangle$ is maximally entangled with $E = \log_2 d \equiv E_d$ if and only if all Schmidt coefficients are equal, $\chi_k = 1/d$, and hence, if and only if the matrix $\sqrt{d}\psi$ is unitary. The number of non-zero Schmidt coefficients is denoted as the Schmidt rank $r = \text{rank}(\psi)$ and may be interpreted as the dimensionality of entanglement [31].

For later use, we briefly apply this measure to a general two-qubit state (of electron spins), expanded in the computational basis as

$$|\phi_{ee}\rangle = \sum_{j_a=0,1} \sum_{j_b=0,1} c_{j_a j_b} |j_a, j_b\rangle. \quad (2)$$

The two Schmidt coefficients are $\sqrt{\lambda_\pm}$ with

$$\lambda_\pm = \frac{1}{2} \pm \sqrt{\frac{1}{4} - (\det \phi_{ee})^2}, \quad \phi_{ee} = \begin{pmatrix} c_{00} & c_{01} \\ c_{10} & c_{11} \end{pmatrix}. \quad (3)$$

The entanglement is $E_{ee} = -\lambda_+ \log_2 \lambda_+ - \lambda_- \log_2 \lambda_-$. Maximal entanglement $E_{ee} = 1$ is obtained for $|\det \phi_{ee}| = 1/2$.

Next we derive an effective action in the nuclear spin space describing one iteration of entanglement transfer, $|\psi_{j_a j_b}^{(\nu)}\rangle = \mathcal{T}_{j_a j_b} |\psi^{(\nu-1)}\rangle$, where $|\psi^{(\nu)}\rangle$ is the nuclear state after iteration ν . Here, the two indices denote the measurement outcomes (j_a, j_b) in round ν , while (for $\nu > 1$) the dependence of the states on the previous measurement outcomes is taken as implicit. We assume that the internode entangling mechanism,

described in Sec. III B, leaves nuclear spins decoupled until successful generation of an entangled state $|\phi_{ee}\rangle$, so here we only need to include the electron-nuclear controlled gate and the X basis measurement of electron spins. In the basis $\{e_a\} \otimes \{e_b\} \otimes \{n_a\} \otimes \{n_b\}$, where, e.g. $\{e_a\} = (|0\rangle, |1\rangle)$ is the basis of the electron spin qubit in node a , the controlled operation $\mathcal{M} = \mathcal{C}(U_{a,0}, U_{a,1}) \otimes \mathcal{C}(U_{b,0}, U_{b,1})$ takes the block-diagonal form,

$$\mathcal{M} = \begin{pmatrix} U_{a,0} \otimes U_{b,0} & & & \\ & U_{a,0} \otimes U_{b,1} & & \\ & & U_{a,1} \otimes U_{b,0} & \\ & & & U_{a,1} \otimes U_{b,1} \end{pmatrix}, \quad (4)$$

with all off-diagonal blocks being zero. To implement the X basis measurement we further apply the electron spin $\pi/2$ rotations, resulting in $(Y^{1/2} \otimes Y^{1/2})\mathcal{M}$. The effective gate $\mathcal{T}_{j_a j_b}$ is obtained by projecting onto the measured $(|j_a, j_b\rangle)$ and initial state $(|\phi_{ee}\rangle)$, prepared, e.g., by a successful photonic scheme attempt of both electron spins from the left and right, respectively,

$$\mathcal{T}_{j_a j_b} = \langle j_a, j_b | (Y^{1/2} \otimes Y^{1/2})\mathcal{M} |\phi_{ee}\rangle. \quad (5)$$

For a general two-qubit state, Eq. (2), we explicitly obtain

$$\mathcal{T}_{j_a j_b} = \frac{1}{2} \sum_{j'_a j'_b} \eta_{j_a j'_a} \eta_{j_b j'_b} c_{j'_a j'_b} U_{a, j'_a} \otimes U_{b, j'_b}, \quad (6)$$

where $\eta_{j_j} \equiv (-1)^{\delta_{j,0} \delta_{j',1}}$. The effective gate $\mathcal{T}_{j_a j_b}$ is in general not unitary. Without normalization, the state resulting from the entanglement transfer is, in matrix notation,

$$\psi_{j_a j_b}^{(\nu)} = \frac{1}{2} \sum_{j'_a j'_b} \eta_{j_a j'_a} \eta_{j_b j'_b} c_{j'_a j'_b} U_{a, j'_a} \psi^{(\nu-1)} U_{b, j'_b}^\top. \quad (7)$$

Note that the subscripts j_a, j_b are never meant as matrix element indices. The probability for obtaining the measurement outcome (j_a, j_b) is given by $P_{j_a j_b}^{(\nu)} = \langle \psi_{j_a j_b}^{(\nu)} | \psi_{j_a j_b}^{(\nu)} \rangle = \text{Tr } \psi_{j_a j_b}^{(\nu)} \psi_{j_a j_b}^{(\nu)\dagger}$ provided $|\psi^{(\nu-1)}\rangle$ has been normalized. The entanglement $E_{j_a j_b}^{(\nu)}$ generally also depends on the measurement outcome; when we omit the measurement outcome indices, we mean the target value $E^{(\nu)}$ that we want to achieve.

B. Transferability conditions

We now derive explicit conditions for achieving the goal of generating maximally entangled states. The term ‘transferability’ is adopted from Ref. [18], where conditions have been formulated for deterministic transfer of $E_{ee} = 1$ to a target qudit pair, irrespective of their Hilbert space dimension. Their condition is formulated in terms of the Schmidt decomposition of the state immediately before the projection(s), which in our case can be written as $\sum_{j_a j_b} |j_a, j_b\rangle \mathcal{T}_{j_a j_b} |\psi^{(\nu-1)}\rangle$, since the different projected electron states form an orthonormal

set. In the least explicit form, the transferability condition states that the Schmidt coefficients are to be preserved by the projection. In this work, we take a slightly different but not necessarily less general approach by formulating conditions for entanglement transfer based on the three-step process described in Sec. II A. Thus, the conditions depend on resource state $|\phi_{ee}\rangle$, conditional operations $\{\mathcal{C}(U_{K,0}, U_{K,1})\}$, and, in the case of postselection, measurement outcomes $\{j_K\}$. The fact that $\{U_{K,0}, U_{K,1}\}$ are unitary operations allows us to formulate more explicit conditions than given in Ref. [18]. Another difference is that we consider entanglement accumulation in finite-dimensional systems, which are to be maximally entangled, and this requires different strategies, at least for some values of d . We further note that the increase of the two-qudit entanglement in one iteration is bound by the consumed resource E_{ee} even in the probabilistic case of postselection, despite the involvement of projections.

To derive the following conditions, we write the state resulting from the previous iteration $\nu - 1$, which for $\nu = 1$ is the initial state, in the Schmidt decomposition

$$|\psi^{(\nu-1)}\rangle = \sum_{k=1}^{r^{(\nu-1)}} \sqrt{\chi_k} |u_k\rangle_a \otimes |u_k\rangle_b. \quad (8)$$

In matrix notation, this reads

$$\psi^{(\nu-1)} = V_a \text{diag}(\{\sqrt{\chi_k}\}) V_b^\top, \quad (9)$$

with semi-unitary $d \times r^{(\nu-1)}$ -dimensional matrices V_K , whose columns correspond to $\{|u_k\rangle_K\}$. The Schmidt coefficients are positive and sorted in decreasing order. The entanglement is $E^{(\nu-1)} = -\sum_k \chi_k \log_2 \chi_k$. Substituting into Eq. (7), one finds that, to increase the rank by $\delta r^{(\nu)} \equiv r^{(\nu)} - r^{(\nu-1)} \geq 0$, it is necessary (and sufficient for $E_{ee} > 0$) that $\delta r^{(\nu)}$ columns of $U_{K,1} V_K$ lie outside the span (column space) of $U_{K,0} V_K$ for $K = a, b$; further one can see that the rank at most doubles, $\delta r^{(\nu)} \leq r^{(\nu-1)}$. Let us define the orthonormal basis Q_K of the subspace spanned by the columns of $U_{K,0} V_K$ and $U_{K,1} V_K$. The first $r^{(\nu-1)}$ columns of Q_K are chosen as $U_{K,0} V_K$, the last $\delta r^{(\nu)}$ columns denoted as V_K^\perp . This allows us to write

$$U_{a,0} \psi^{(\nu-1)} U_{b,0}^\top = Q_a \sqrt{S_\downarrow} Q_b^\top, \quad (10)$$

where $\sqrt{S_\downarrow} = \text{diag}(\{\sqrt{\chi_k}\}) \oplus 0_{\delta r^{(\nu)}}$ is the direct sum of the diagonal matrix of the singular values with a zero matrix of size $\delta r^{(\nu)}$; the down arrow indicates the decreasing order of the diagonal elements. According to Eq. (7), the column (row) space of $\psi_{j_a j_b}^{(\nu)}$ lies in the span of Q_a (Q_b), so we can write

$$\psi_{j_a j_b}^{(\nu)} = Q_a \tilde{\psi}_{j_a j_b}^{(\nu)} Q_b^\top \quad (11)$$

with $\tilde{\psi}_{j_a j_b}^{(\nu)} \equiv Q_a^\dagger \psi_{j_a j_b}^{(\nu)} Q_b^*$. Explicitly, we obtain

$$\psi_{j_a j_b}^{(\nu)} = \frac{1}{2} \sum_{j'_a j'_b} \eta_{j_a j'_a} \eta_{j_b j'_b} c_{j'_a j'_b} U_{a, j'_a} \sqrt{S_\downarrow} U_{b, j'_b}^\top \quad (12)$$

with $\mathcal{U}_{K,j} \equiv Q_K^\dagger U_{K,j} U_{K,0}^\dagger Q_K$. Now, since $\mathcal{U}_{K,0} = \mathbb{1}_{r^{(\nu)}}$, we define $\mathcal{U}_K \equiv \mathcal{U}_{K,1}$ and write out the sum as

$$\begin{aligned} \tilde{\psi}_{j_a j_b}^{(\nu)} &= \frac{1}{2} \left(c_{00} \sqrt{S_\downarrow} - (-1)^{j_b} c_{01} \sqrt{S_\downarrow} \mathcal{U}_b^\top \right. \\ &\quad \left. - (-1)^{j_a} c_{10} \mathcal{U}_a \sqrt{S_\downarrow} + (-1)^{j_a} (-1)^{j_b} c_{11} \mathcal{U}_a \sqrt{S_\downarrow} \mathcal{U}_b^\top \right). \end{aligned} \quad (13)$$

The matrix \mathcal{U}_K is unitary in general only for $r^{(\nu)} = d$.

1. Deterministic complete entanglement transfer

The necessary and sufficient condition for the complete deterministic transfer of E_{ee} is that in each node the two gates $U_{K,j}$ generate out of the previous Schmidt vectors (the columns of V_K) two mutually orthogonal sets of $r^{(\nu-1)}$ vectors (which implies $\delta r^{(\nu)} = r^{(\nu-1)}$, thus $r^{(\nu)}$ even), which can be expressed as

$$V_K^\dagger U_{K,0}^\dagger U_{K,1} V_K = 0, \quad (14)$$

for $K = a, b$. An equivalent formulation is

$$S_\downarrow \mathcal{U}_K S_\downarrow = 0. \quad (15)$$

To prove both directions, we note that in this case only can we choose $V_K^\perp = U_{K,1} V_K$. Then, \mathcal{U}_K is block-antidiagonal with the lower left block given by the identity matrix $\mathbb{1}_{r^{(\nu-1)}}$. The state from Eq. (13) becomes

$$\tilde{\psi}_{j_a j_b}^{(\nu)} = \frac{1}{2} \left[\begin{pmatrix} -1 & 0 \\ 0 & (-1)^{j_a} \end{pmatrix} \phi_{ee} \begin{pmatrix} -1 & 0 \\ 0 & (-1)^{j_b} \end{pmatrix} \right] \otimes \text{diag}(\{\sqrt{\lambda_k}\}). \quad (16)$$

The matrices with sign factors are just basis vector inversions and do not affect the singular values. The tensor product structure shows that the Schmidt coefficients of $|\psi^{(\nu)}\rangle$ are given by pairwise products of that of $|\phi_{ee}\rangle$ and $|\psi^{(\nu-1)}\rangle$, i.e., each $r^{(\nu-1)}$ Schmidt coefficients $\{\sqrt{\lambda_{+}\chi_k}\}$ and $\{\sqrt{\lambda_{-}\chi_k}\}$ with λ_{\pm} given in Eq. (3). Straightforward algebra then shows that the entanglement, defined in Eq. (1), is given by $E^{(\nu)} = E^{(\nu-1)} + E_{ee}$.

This type of entanglement transfer has the following properties: (i) It works independently of the choice of entanglement resource state $|\phi_{ee}\rangle$ (with $E_{ee} > 0$) and also comes without any explicit constraints on the values of the $r^{(\nu-1)}$ Schmidt coefficients, apart from $r^{(\nu-1)} \leq \lfloor d/2 \rfloor$. (ii) The norm of the state $|\psi_{j_a j_b}^{(\nu)}\rangle$ is $1/2$, which means that the probabilities of individual measurement outcomes are equal, $P_{j_a j_b}^{(\nu)} = 1/4$. (iii) If during the conditional operation $C(U_{K,0}, U_{K,1})$ a single-qubit Z gate is applied on the electron spin e_K , this amounts to multiplying the Schmidt vectors of $|\psi_{j_a j_b}^{(\nu)}\rangle$ with phases, which does not affect the complete transfer.

Since Eq. (14) is a necessary condition but requires $r^{(\nu)}$ to be even, it is impossible to generate an odd Schmidt rank $r^{(\nu)}$ by a complete deterministic transfer. This includes the generation of an odd-ranked maximally entangled state. It

might still be possible to achieve the latter goal by an incomplete deterministic transfer; the corresponding conditions are given in the next subsection (Sec. II B 2). Otherwise, only probabilistic entanglement transfer remains as an option to generate odd-ranked maximal entanglement. Note that in the case of postselection, a complete but probabilistic entanglement transfer may be realized even when the operations $C(U_{K,0}, U_{K,1})$ do not have full entangling capacity, as opposed to condition (14); this fact is closely related with entanglement concentration through probabilistic entanglement swapping proposed in Ref. [32].

2. Deterministic generation of maximal entanglement

Consider now the final iteration in which a maximally entangled state, $E^{(\nu)} = E_d$, is to be generated. If $E^{(\nu-1)} = E_d - 1$, then, apart from the need $E_{ee}^{(\nu)} = 1$, the situation is equivalent with that considered in Sec. II B 1, and the necessary and sufficient condition is Eq. (14). Here we thus consider $E^{(\nu-1)} > E_d - 1$, and hence, $r^{(\nu-1)} > d/2$. In Appendix A we derive the following items as necessary and sufficient conditions:

- (1) $|\phi_{ee}^{(\nu)}\rangle$ is maximally entangled, i.e., $E_{ee}^{(\nu)} = 1$. (Thus, the entanglement transfer is incomplete.)
- (2) The diagonal elements of S_\downarrow , consisting of Schmidt coefficients and zeros, come in pairs $1/d \pm \varepsilon_i$ with $0 \leq \varepsilon_i \leq 1/d$, for $i = 1, \dots, \lfloor d/2 \rfloor$, and one further unpaired central element $1/d$ in the case of odd d . Groups of identical successive diagonal elements of S_\downarrow are termed blocks.
- (3) The unitary matrix \mathcal{U}_K (for $K = a, b$) has a corresponding block-antidiagonal structure. This yields an explicit condition for the physical interaction U_K , since the transformation Q_K relating the two matrices is for $r^{(\nu)} = d$ uniquely determined, apart from trivial operations (phases/reordering) within subspace V_K^\perp .
- (4) Two further constraints on $\{\mathcal{U}_K\}$ described by Eqs. (A8), which can be further simplified depending on $r^{(\nu-1)}$ and the choice of $|\phi_{ee}^{(\nu)}\rangle$.

Note that constraint (2) implies that $\delta r^{(\nu)}$ Schmidt coefficients must be equal to $2/d$, and further, that is impossible to deterministically generate maximal entanglement for odd d when the previous state is even-ranked with equal Schmidt coefficients. Therefore, a strategy derived from these constraints, which covers only the final iteration, cannot be combined with a scheme for the first iterations derived from Sec. II B 1, to give a complete scheme for odd d .

III. MODEL OF THE QUANTUM NETWORK

The concept of entanglement transfer is known to be applicable to both defect centers with central nuclear spin [17]

and with weakly coupled nuclear spins [33]. In order to apply the concept in the version generalized to higher-dimensional memory qudits, we define an explicit physical model of a quantum network node as a defect center with higher nuclear spin in Sec. III A. A known mechanism for entangling two such nodes is described in Sec. III B.

A. Single node: Defect center

A defect center with one central electron and one nuclear spin serves as a node, and we assume that no further strongly coupled spins are nearby. Decoherence is not included as we focus on the basic principle. This is also to a good degree justified from the time scales: the node-node entangling mechanism (e.g., photon-based) is much faster than electron spin coherence times, and the hyperfine coupling to the central nuclear is typically dominant and its inverse much shorter than nuclear spin coherence times. We further assume that a magnetic field B is applied along the symmetry axis of the defect, which is taken as the z axis. The Hamiltonian of the node is composed of electron, nuclear, and hyperfine parts,

$$H = H_e + H_n + H_{\text{hf}}. \quad (17)$$

The electron part H_e may contain several contributions depending on the type of defect center and crystal. In this Section, we describe the simplest case without additional contributions such as strain and orbital degree of freedom, which are treated for other defect centers in Appendix B. The model discussed here is applicable to an ideal NV center and to implanted group-V donors in silicon, and is referred to as NV-type center. In this model, the electron part only contains the quadrupole (for electron spin quantum number $S > 1/2$) and the Zeeman terms,

$$H_e = DS_z^2 + \gamma_e BS_z. \quad (18)$$

The terms in the nuclear-spin Hamiltonian are analogous to that of H_e , but by contrast to Eq. (18) are universal to all types of defect centers,

$$H_n = QI_z^2 - \gamma_n BI_z, \quad (19)$$

with parameters Q and γ_n depending on the nuclear isotope.

We consider high-symmetry defects, where the hyperfine tensor is approximately diagonal with $A_{xx} = A_{yy} = A_{\perp}$ and $A_{zz} = A_{\parallel}$,

$$H_{\text{hf}} = A_{\parallel} S_z I_z + \frac{A_{\perp}}{2} (S_+ I_- + S_- I_+), \quad (20)$$

where $S_{\pm} = S_x \pm iS_y$, $I_{\pm} = I_x \pm iI_y$. Since the hyperfine coupling between the central spins is mainly due to the Fermi contact interaction, the two components A_{\parallel} and A_{\perp} are of the same order of magnitude; for donor spins in silicon, they are often taken as identical [16].

In analogy to the spin-1/2 scheme of Refs. [17, 34], we use the Ising component A_{\parallel} for the entanglement transfer. The exchange part A_{\perp} as well as the off-diagonal terms in H_e may

be suppressed by choosing the two electron qubit levels sufficiently separate in energy from neighboring levels in terms of the magnetic quantum number. This is usually achieved by tuning B and reduces the undesirable terms to dispersive level shifts. We discuss this in more detail for two types of defects in Appendix B. In Appendix C we show explicitly for the NV center in diamond that the influence of this correction on the generated entanglement is very small and may be safely neglected. With this secular approximation applied, we are left with an interaction term, $H_{\text{hf}} = A_{\parallel} S_z I_z$.

The nuclear part H_n is diagonal and thus commutes with H_{hf} , which is the only way in which the nuclear spins are operated on. This means that H_n only generates a single-qudit gate that does not influence the entanglement E between remote nuclear spins. More precisely, if we consider the full hyperfine interaction (20), there is a correction which is quadratic in A_{\perp} but so small that it may be safely neglected.

We assign the electron qubit states $|0\rangle$ and $|1\rangle$ to the magnetic quantum numbers m_s and m'_s , respectively, and assume that all other electron levels remain unoccupied throughout. Thus, we can write the Hamiltonian as $H = |0\rangle\langle 0| \otimes h_0^{\text{eff}} + |1\rangle\langle 1| \otimes h_1^{\text{eff}}$, where h_j^{eff} are two effective conditional Hamiltonians for the nuclear spin. If $m_s + m'_s \neq 0$, we can simplify the expressions, without affecting the entanglement, by choosing a symmetrizing nuclear spin rotating frame defined by the time-dependent basis change $U(t) = \exp[-i(m_s + m'_s)A_{\parallel}I_z t/2\hbar]$. In this way, we obtain

$$h_j^{\text{eff}} = (-1)^j (A_{\text{net}} I_z + \Delta I_0)/2, \quad A_{\text{net}} \equiv (m_s - m'_s)A_{\parallel}, \quad (21)$$

where Δ is the energy difference between levels m_s and m'_s . We assign the qubit states such that $A_{\text{net}} > 0$. For $S = 1/2$ or any two consecutive levels of a higher spin manifold, $A_{\text{net}} = |A_{\parallel}|$, while otherwise, A_{net} is amplified but without any fundamental advantage (i.e., extension of control possibilities) compared to the $S = 1/2$ case. Adding a node index K , the time-evolution operators corresponding to h_j^{eff} are

$$U_{K,j} = \tilde{Z}_{K,(-1)^j \varphi_K}, \quad \tilde{Z}_{K,\varphi_K} \equiv \exp(-i\varphi_K(I_z + \xi_K I_0)/2), \quad (22)$$

where $\varphi_K \equiv A_{\text{net},K}t/\hbar$ and $\xi_K \equiv \Delta_K/A_{\text{net},K}$. The dynamics of the electron-nuclear system is thus described by the CPHASE-like gate $|0\rangle\langle 0| \otimes \tilde{Z}_{K,\varphi_K} + |1\rangle\langle 1| \otimes \tilde{Z}_{K,-\varphi_K}$. In the hypothetical case $\xi_K = 0$, the operator \tilde{Z}_{K,φ_K} reduces to the Z rotation (Z_{φ_K}). The electronic level difference Δ_K is typically in the GHz regime and may in general cause undesirable rapid oscillations in the entanglement transferred onto the nuclear spins as a function of φ_K . Switching to a rotating frame for the electron spin as done in Refs. [17, 34] does not remove these oscillations since the measurement needs to be carried out in the laboratory frame. The points of complete deterministic entanglement transfer are unaffected by the oscillations (i.e., independent of the precise value of ξ_K) due to property (iii) derived in Sec. II B 1; an additional exception is discussed in the next subsection.

B. Entangling nodes

For defect centers featuring a spin-photon interface, single-photon interference may be the preferred way of projecting electron spins in distant nodes into an entangled state. Any other entangling mechanism which is capable of keeping nuclear spin qudits decoupled is explicitly allowed. For our purpose it just matters which state $|\phi_{ee}\rangle$ with $E_{ee} = 1$ is produced. Even though complete deterministic entanglement transfer is unaffected by this choice, it is relevant for other transfer types and for the nuclear spin state being generated. Note that while photon-mediated interactions between higher-dimensional spin systems are conceivable [35], in this work we use the electron spins as qubits and correspondingly the spin-photon interface in the traditional binary fashion with two outcomes, e.g., reflection or no reflection of the photon.

The photonic scheme has been described in Ref. [17] and analyzed in more detail for both the NV center and a group-IV (silicon) vacancy in diamond in Ref. [36]. Here we assume a perfect photonic scheme without any losses in the channels and with perfect contrast of the spin-dependent reflection. We consider the Mach-Zehnder interferometer setup shown in blue in Fig. 1. It consists of a single-photon source, a 50:50 beam splitter, the spin-photon interface of each node, another 50:50 beam splitter (which in a two-way setup would coincide with the first one), and a single-photon detector. We assume that the photon is reflected (with an irrelevant phase shift π) if the cavity's electron spin (stationary qubit) is in state $|0\rangle$, while it is lost (scattered) for the other qubit state $|1\rangle$. In neither case a change to the stationary qubit occurs. Initially, each stationary qubit is in one of the two superposition states $|\pm\rangle = (|0\rangle \pm |1\rangle)/\sqrt{2}$. Without loss of generality, we may consider one of them to be in $|+\rangle$; in particular, we consider the initial state $|+\pm\rangle_{e_a e_b}$. In the following, we use the notation $|ph_1 ph_2 e_a e_b\rangle$ for the state of both flying and stationary qubits, where '1' and '2' are the photonic channels on the left and right side of the beam splitter, respectively. The (photon amplitude) number $ph_i \in \{0, 1\}$ describes the absence/presence of a photon in channel i . A single photon is incident in channel 1, so the entire initial state is $|10+\pm\rangle$. After scattering from the beam splitter, the state is path-entangled, $\frac{1}{\sqrt{2}}(|10+\pm\rangle + |01+\pm\rangle)$. The photon modes now interact with the corresponding cavities which yields $\frac{1}{\sqrt{2}}(|100\pm\rangle + |01+0\rangle)$. Here we omitted two further terms for which no photon is reflected from either cavity. Effectively this is realized by a post-selection of outcomes with detector click events. Now, the reflected photon parts interfere at the second beam splitter, which destroys the which-path information and leads to $\frac{1}{2}(|100\pm\rangle - |010\pm\rangle + |01+0\rangle + |10+0\rangle)$. Here, a π phase shift occurs for transmission from the upper left to the lower right channel (but could be at any other scattering matrix element). Finally, by selecting outcomes where the detector at the dark port (channel 2) clicks, the stationary qubits are projected into the state $|\Psi^\pm\rangle$, where

$$|\Psi^\pm\rangle = \frac{1}{\sqrt{2}}(|01\rangle \pm |10\rangle). \quad (23)$$

This state can be transformed into any other maximally entan-

gled state by local operations. In particular, one of the other two Bell states

$$|\Phi^\pm\rangle = \frac{1}{\sqrt{2}}(|00\rangle \pm |11\rangle) \quad (24)$$

is obtained by driving one spin qubit with a π -pulse. On the other hand, driving with a $\pi/2$ -pulse yields a two-qubit cluster state, e.g.,

$$|\Phi_C\rangle = \frac{1}{\sqrt{2}}(|0+\rangle + |1-\rangle) = \frac{1}{\sqrt{2}}(|\Phi^-\rangle + |\Psi^+\rangle). \quad (25)$$

As a side note, if the naturally obtained state $|\Psi^\pm\rangle$ is used, the entangled state preparation (excluding initialization) commutes with the electron-nuclear controlled gate, while with driving it does not.

The probability for the detector to click, i.e., for entangling the remote electron spins, is $1/8$. Thus the photonic scheme is repeated until success (dash-dotted box in Fig. 1) in each iteration of entanglement transfer (dashed box in Fig. 1). When we give probabilities for the iterative entanglement transfer scheme in Sec. IV, we do not include the photonic scheme probability, which simply multiplies to the overall probability. We further note that an alternative photonic scheme has been proposed [36], which generates a maximally entangled state deterministically. The key difference is that the phase instead of the amplitude of the cavity-reflected photon is dependent on the electron spin, with the downside of not allowing a quantum non-demolition measurement of the qubit state without making use of an interferometer.

The photonic scheme described above naturally results in one of the Bell states $|\Psi^\pm\rangle$. Substituting this state along with evolution operators (22) into the effective gate (6), one can see that the typically large parameter ξ drops out from the nuclear spin evolution and entanglement, provided ξ is identical for both nodes. For all other states $|\phi_{ee}\rangle$, the generated qudit entanglement typically oscillates rapidly as a function of the CPHASE angle φ , except at points of complete deterministic transfer (see property (iii) in Sec. II B 1). In Ref. [17] ($d = 2$), the two-qubit cluster state $|\phi_{ee}\rangle = |\Psi_C\rangle \equiv (|0+\rangle + |1-\rangle)/\sqrt{2}$ was chosen as the resource with the goal of generating a nuclear spin cluster state; here we briefly note that the generated state depends on ξ and is a two-qubit cluster state up to local Z rotations (for any measurement outcome) only for 2ξ integer and odd, which could be achieved by fine tuning B [37].

IV. ENTANGLEMENT ACCUMULATION

In this section, we consider two nodes and explore schemes to accumulate entanglement between the nuclear spin qudits via the Ising coupling to their respective electron spins. Each node is effectively characterized by the coupling strength A_{net} and the transition energy Δ . By default, all nuclear spin levels are used to define the qudit so that $d = 2I + 1$, but it is possible to deliberately lower the dimension by leaving levels unoccupied at one end (or both ends) of the magnetic ladder. Then the occupied levels up to a rotating frame evolve equivalently to a nuclear spin with the corresponding level number.

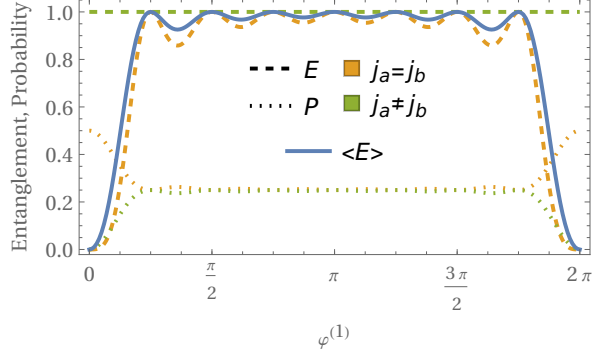


FIG. 2. First iteration of entanglement transfer ($d = 8$, $|\phi_{ee}\rangle = |\Psi^+\rangle$), showing entanglement and probability for individual measurement outcomes (j_a, j_b) as well as the expected entanglement, as functions of the CPHASE angle.

This gives the opportunity to define from nuclear spin I a qudit with dimension $d = 2^{\lfloor \log_2(2I+1) \rfloor}$, which, as shown in Sec. IV A, is suitable for deterministic entanglement accumulation. As an example, a $d = 8$ qudit may be defined from the $I = 9/2$ spin of ^{73}Ge by leaving the two levels $m_I = \pm 9/2$ empty. The only disadvantage is possible leakage into the unoccupied levels especially during driving operations, causing lower fidelities. An alternative but more profound modification is defining a qudit from the electron spin (provided its quantum number is $S > 1/2$), which, for the same coupling $S_z I_z$, would alter the set of favorable qudit dimensions d accordingly, since the base two in 2^n is the qubit dimension.

Since the rotation axis is fixed throughout and no other (driving) operations are applied, the effective gates ($\{\mathcal{T}^{(\nu)}\}$) commute with each other, so that generally the order in which the phases $\{\varphi^{(\nu)}\}$ are applied does not affect the final state. The rank doubles in each iteration ($r^{(\nu)} = 2r^{(\nu-1)}$) or reaches the maximum ($r^{(\nu)} = d$), whenever we apply a phase $\varphi^{(\nu)}$ that has not been applied in one of the previous iterations; otherwise the rank remains the same or even decreases. (If $|\phi_{ee}^{(\nu)}\rangle \neq |\phi_{ee}^{(\nu')}\rangle$, then only discrete values of $\varphi^{(\nu)} = \varphi^{(\nu')}$ do not double the rank.)

The state $|\psi_J^{(\nu)}\rangle$ after ν iterations depends on the 2ν measurement outcomes $J \equiv \{j_a^{(\mu)}, j_b^{(\mu)} | \mu = 1, \dots, \nu\}$ and its entanglement $E_J^{(\nu)}$ may in general also depend on the measurement record J . Of interest is the expectation value of the entanglement, $\langle E^{(\nu)} \rangle = \sum_J P_J E_J^{(\nu)}$, with $P_J = \langle \psi_J^{(\nu)} | \psi_J^{(\nu)} \rangle$. Without giving a proof, we note that $\langle E^{(\nu)} \rangle$ is 2π -periodic in any $\varphi^{(\nu)}$ and for any ξ . In the following, we omit the measurement outcome index J for ease of notation.

A. Constructed deterministic entanglement transfer scheme

A unique property of quantum spin is that the rotation around a fixed axis can generate a complete orthonormal set of states from a single, suitably chosen, state vector. More specifically, for the essential z -axis rotation \tilde{Z}_{K, φ_K} , Eq. (22), the necessary and sufficient requirement is that the initial state

is uniform in the eigenbasis of I_z (i.e., each component has square modulus $1/d$), and the rotation angles form the cyclic group, $\varphi_k = 2\pi k/d$, with integer k . We can thus exploit a conditional I_z rotation to implement a simple realization of repeated complete deterministic entanglement transfer. For this, the initial nuclear two-qudit state needs to be chosen as

$$|\psi^{(0)}\rangle = |+_d\rangle \otimes |+_d\rangle, \quad |+_d\rangle \equiv \frac{1}{\sqrt{d}} \sum_{i=0}^{d-1} |i\rangle. \quad (26)$$

For the first iteration, the orthogonality condition (14) is $\langle +_d | \tilde{Z}_{K, 2\varphi_K^{(1)}} | +_d \rangle = 0$ and yields $\varphi_K^{(1)} = k2\pi/d$ with integer $k \in \{1, \dots, d-1\}$. Choosing $\varphi_a^{(\nu)} = \varphi_b^{(\nu)} \equiv \varphi^{(\nu)}$, the plot in Fig. 2 confirms for $d = 8$ and $|\phi_{ee}\rangle = |\Psi^+\rangle$ that the expected entanglement reaches 1 ebit for these angles. The individual probabilities $P_{j_a j_b}$ and entanglements $E_{j_a j_b}$ are also shown; note that $E_{01} = E_{10} = 1$ for any $\varphi^{(1)}$. The plots for other d are analogous.

For any of the later iterations ν we use that the transfer of 1 ebit has been deterministically achieved in each previous iteration by choosing suitable angles $\{\varphi^{(\mu)}\}$, so that the Schmidt rank of $|\psi^{(\nu-1)}\rangle$ is $r^{(\nu-1)} = 2^{\nu-1}$. This further implies that for each node K , the $2^{\nu-1}$ states,

$$|v_{\{\sigma(\dots)\}}^{(\nu-1)}\rangle_K = \tilde{Z}_{\sigma^{(\nu-1)} \varphi^{(\nu-1)}} \dots \tilde{Z}_{\sigma^{(1)} \varphi^{(1)}} |+_d\rangle, \quad (27)$$

with sign factors $\sigma^{(\mu)} = \pm 1$ are an orthonormal set with the same span as the Schmidt basis for $|\psi^{(\nu-1)}\rangle$. Thus we can express the single-node condition (14) as

$$_K \langle v_{\{\sigma(\dots)\}}^{(\nu-1)} | \tilde{Z}_{K, 2\varphi^{(\nu)}} | v_{\{\sigma(\dots)\}}^{(\nu-1)} \rangle_K = 0, \quad (28)$$

which must hold for any of the $2^{2\nu-2}$ combinations of sign factors. Since the parameter ξ_K only causes scalar phase factors, it drops out from the condition as expected for a complete deterministic transfer. Explicit evaluation yields

$$\sum_{k=-I}^I \exp \left[-ik \left(\varphi^{(\nu)} + \sum_{\mu=1}^{\nu-1} \tau^{(\mu)} \varphi^{(\mu)} \right) \right] = 0, \quad (29)$$

for all combinations of $\{\tau^{(\mu)}\}$, where $\tau^{(\mu)} \in \{-1, 0, 1\}$. With $\tau^{(\mu)} = 0$ for all μ , we obtain the same phase discretization as for the first iteration, $\varphi^{(\nu)} = k^{(\nu)} 2\pi/d$ with integer $k^{(\nu)} \in \{1, \dots, d-1\}$. The other combinations further restrict the allowed indices $k^{(\nu)}$. For the second iteration, we find the constraints $k^{(2)} \neq k^{(1)}$ and $k^{(2)} \neq d - k^{(1)}$. Any number up to $\nu_{\max} = \lfloor E_d \rfloor$ of maximal transfer iterations can be realized by the set of indices $k^{(\nu)} = 2^{\nu-1}$, which is also the set with the shortest gate duration. Thus, with each $|\phi_{ee}^{(\nu)}\rangle$ providing 1 ebit, the phase set

$$\varphi^{(\nu)} = \frac{2^\nu \pi}{d}, \quad \nu = 1, \dots, \nu_{\max}, \quad \nu_{\max} = \lfloor E_d \rfloor \quad (30)$$

deterministically results in $E = \lfloor E_d \rfloor$, which corresponds to the maximal entanglement E_d for the case $d = 2^n$ with any integer n . The order in which the phases $\{\varphi^{(\nu)}\}$ are applied,

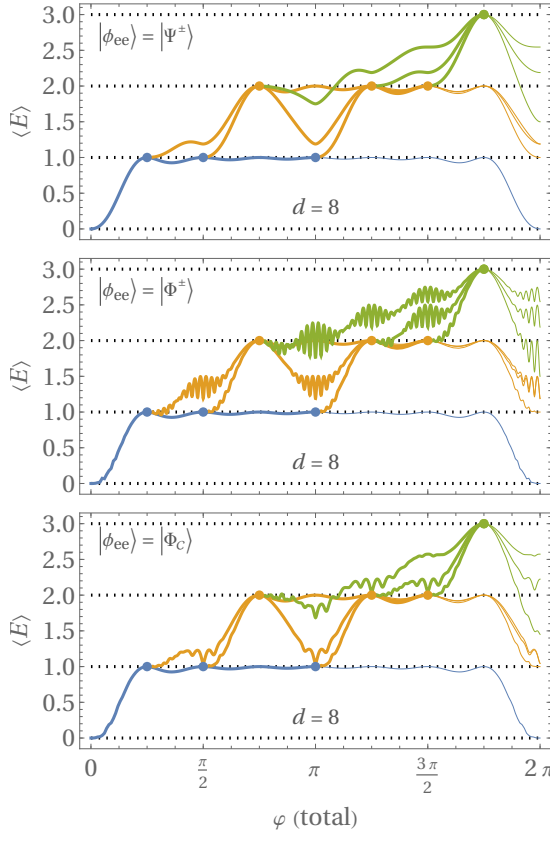


FIG. 3. Generating maximal entanglement deterministically in three iterations for $d = 8$. The expected entanglement without postselection is shown as a function of the accumulated CPHASE angle. Only the fastest phase combinations are shown (set (30), any ordering).

does not matter, and could also differ between the two nodes, but this would result in a longer total duration.

The plots in Fig. 3 confirm that this phase set indeed leads to a deterministic increase of the entanglement by 1 ebit in each iteration, for all choices of (maximally entangled) $|\phi_{ee}\rangle$. This deterministic increase is possible until $E = \lfloor E_d \rfloor$ is reached. The total CPHASE angle required to achieve this is smaller than 2π (e.g., $\varphi = 7\pi/4$ for $d = 8$ shown in Fig. 3).

Not surprisingly, the bipartite entanglement generated by such a series of 1-ebit transfers is decomposable [38], i.e., the correlations are reproducible by n pairs of qubit Bell pairs. This is not the case for the remaining schemes based on incomplete transfers, nor does it generalize to the multipartite case (Sec. V). Furthermore, this property should not necessarily be considered a downside for quantum computing tasks.

For qudits with $d \neq 2^n$ we require at least $\nu_{\max} = \lceil E_d \rceil$ iterations to reach $E = E_d$, but the constraints implied by Eq. (29) cannot be fulfilled for any further iteration, $\nu > \lfloor E_d \rfloor$. It further turns out that, in agreement with the deviating constraints for generating maximal entanglement deterministically (Sec. II B 2), after such $\lfloor E_d \rfloor$ iterations of deterministic transfer we are in a bad position for further increasing the ex-

pected entanglement significantly (e.g., for some d the entanglement directly decreases from this point). Reaching higher values of entanglement for such qudit dimensions requires other schemes, which are identified in the following subsections; in particular, we don't find a method without driving that achieves (near-) maximal entanglement deterministically.

B. Constructed entanglement transfer scheme ($d = 3$)

We now consider the lowest unfavorable qudit dimension, $d = 3$, and investigate whether maximal entanglement can be generated deterministically in some other way. A scheme for $d = 3$ might also be useful as an elementary block of a scheme for (even) multiples of $d = 3$. It is plausible to follow a reverse engineering approach by first applying the constraints derived in Sec. II B 2 for the final iteration. For $d = 3$, the controlled gate $C(U_{K,0}, U_{K,1})$ is described by

$$U_{K,0}^\dagger U_{K,1} = e^{i\xi_K \varphi_K} \begin{pmatrix} e^{i\varphi_K} & 0 & 0 \\ 0 & 1 & 0 \\ 0 & 0 & e^{-i\varphi_K} \end{pmatrix}. \quad (31)$$

We denote the index of the final iteration by ν_f . Due to the constraints on the Schmidt coefficients (item 2 from Sec. II B 2), we have

$$S_\downarrow^{(\nu_f-1)} = \begin{pmatrix} \frac{1}{3} + \varepsilon & 0 & 0 \\ 0 & \frac{1}{3} & 0 \\ 0 & 0 & \frac{1}{3} - \varepsilon \end{pmatrix} \quad (32)$$

with $0 < \varepsilon \leq 1/3$. Only single element blocks are present, and thus, unitary \mathcal{U}_K has the antidiagonal structure,

$$\mathcal{U}_K = \begin{pmatrix} 0 & 0 & e^{i\alpha_+} \\ 0 & e^{i\alpha_0} & 0 \\ e^{i\alpha_-} & 0 & 0 \end{pmatrix}, \quad (33)$$

with yet arbitrary phases. Since $U_{K,0}^\dagger U_{K,1}$ and \mathcal{U}_K are related by the unitary transformation Q_K , their eigenvalues must be identical. The three eigenvalues of \mathcal{U}_K are $\{\pm e^{i(\alpha_+ + \alpha_-)/2}, e^{i\alpha_0}\}$. There are two solutions, namely

$$\mathcal{U}_K = e^{i\xi_K \pi/2} \begin{pmatrix} 0 & 0 & e^{i\alpha_K} \\ 0 & 1 & 0 \\ -e^{-i\alpha_K} & 0 & 0 \end{pmatrix} \wedge \varphi_K = \frac{\pi}{2}, \quad (34)$$

and

$$\mathcal{U}_K = e^{i\xi_K \pi} \begin{pmatrix} 0 & 0 & e^{i\alpha_K} \\ 0 & -1 & 0 \\ e^{-i\alpha_K} & 0 & 0 \end{pmatrix} \wedge \varphi_K = \pi, \quad (35)$$

each containing one arbitrary phase angle α_K . So far we can choose any combination of the two solutions for the two nodes. The remaining constraints from Sec. II B 2 are $E_{ee}^{(\nu)} = 1$ and Eqs. (A8). The constraints from Eqs. (A8) are least restrictive if we choose $\varepsilon = 1/3$. As we will see, this still fixes the state from the previous iteration (up to a phase factor), so that it is not necessary to evaluate the case $\varepsilon < 1/3$,

in which at least one additional iteration would be required ($\nu_f \geq 3$) because $r^{(\nu_f-1)} = 3$, which only lowers the success probability. Thus, we now take $\varepsilon = 1/3$. The upper left and lower right element (block) on the l.h.s. of both Eqs. (A8) then vanish, which yields $P_{eq}^{(\nu_f)} = 1/2$. The central element of the two solutions for \mathcal{U}_K is $\pm e^{i\xi_K \varphi_K}$. Since this is a scalar, the l.h.s. of Eq. (A8a) also vanishes for the central block. The remaining condition from the central block of Eq. (A8b) becomes

$$c^2 \cos(\xi_a \varphi_a + \xi_b \varphi_b) - (\frac{1}{2} - c^2) \cos(\xi_a \varphi_a - \xi_b \varphi_b) = 0. \quad (36)$$

Depending on the values of ξ_a and ξ_b , this equation typically has zero or one solution for c within the allowed range ($0 \leq c \leq 1/\sqrt{2}$), except at discrete points where all allowed c yield a solution. Below we will give an argument for choosing the solution (34) in both nodes, so $\varphi_a = \varphi_b = \pi/2$; in this case, the discrete points are at: one ξ_K integer and even, and the other ξ_K integer and odd. For simplicity we now take $\xi_a = \xi_b \equiv \xi$, which seems to be the most relevant practical case. In this case (and still $\varphi_a = \varphi_b = \pi/2$), Eq. (36) has one (and only one) solution if ξ is not farther away from an even number than $1/2$ (i.e., $|\xi \bmod 2 - 1| \geq 1/2$). If we consider integer and even ξ , then the solution is $c = 1/2$, which means that $|\phi_{ee}^{(2)}\rangle$ is a two-qubit cluster state.

The chosen solutions (out of (34) and (35)) for the two nodes are sufficient to essentially fix the state $|\psi^{(\nu_f-1)}\rangle$ prior to the final iteration. From Eq. (10), $\psi^{(\nu_f-1)} = Q_a \sqrt{S_\downarrow} Q_b^\top$. Since $U_K = Q_K \mathcal{U}_K Q_K^\dagger$ is diagonal, the columns of Q_K^\dagger are the ordered eigenvectors of \mathcal{U}_K . The effective gate $\mathcal{T}_{j_a j_b}$ is also diagonal, which allows us to inspect the possibility of reaching the state $|\psi^{(1)}\rangle$ from a product state $|\psi^{(0)}\rangle$ in the first iteration. (It is fairly obvious that using more than one iteration to generate $|\psi^{(\nu_f-1)}\rangle$ must further lower the success probability, hence we now set $\nu_f = 2$.) It turns out that the structure of $|\psi^{(1)}\rangle$ (in particular, the positions of the vanishing elements) is fitting to the model only if we choose the solution (34) in both nodes, and this choice yields

$$\psi^{(1)} = \frac{1}{\sqrt{6}} \begin{pmatrix} -1 & 0 & 1 \\ 0 & \sqrt{2}e^{i(\alpha_a + \alpha_b)} & 0 \\ 1 & 0 & -1 \end{pmatrix}. \quad (37)$$

Despite the phase freedom at the central element, the state $|\psi^{(1)}\rangle$ seems too strongly constrained to be capable of being generated by entanglement transfer. Thus, a deterministic scheme appears to be unavailable, and we need to rely on postselection in the first iteration.

Instead of performing a general construction, we now use the observation that Bell states are the suitable resource to generate the state given in Eq. (37) in the first iteration. More specifically, we choose $|\phi_{ee}^{(1)}\rangle = |\Psi^+\rangle$, select $\varphi_a^{(1)} = \varphi_b^{(1)} = \pi$, and postselect $j_a = j_b$; other options are given below. It is convenient to partition the d^2 diagonal elements of \mathcal{T}_{jj} into a d by d matrix, explicitly

$$[\text{diag}(\mathcal{T}_{jj})]_{\text{mat}} = \frac{1}{\sqrt{2}} \begin{pmatrix} 1 & 0 & -1 \\ 0 & 1 & 0 \\ -1 & 0 & 1 \end{pmatrix}, \quad (38)$$

so that $\psi^{(1)} \sqrt{P_{jj}} = [\text{diag}(\mathcal{T}_{jj})]_{\text{mat}} \odot \psi^{(0)}$, where \odot is elementwise multiplication, and $\psi^{(\nu)}$ are normalized. The effective gate described by Eq. (38) has a compatible structure with the state from Eq. (37). In particular, the state $|\psi^{(1)}\rangle/2$ (with norm 1/2) is generated by \mathcal{T}_{jj} from the product state

$$\psi^{(0)} = \frac{1}{2\sqrt{3}} (1 \ -\sqrt{2}e^{i(\alpha_a + \alpha_b)} \ 1) \otimes \begin{pmatrix} 1 \\ 1 \\ 1 \end{pmatrix}. \quad (39)$$

Since both outcomes with $j_a = j_b$ are allowed, resulting in the same state up to an irrelevant global phase, the success probability is 1/2. We can summarize the entire scheme, with the parameter ξ tuned to an even integer number, as follows,

$$|\phi_{ee}^{(1)}\rangle = |\Psi^+\rangle, \quad \varphi_a^{(1)} = \varphi_b^{(1)} = \pi, \quad j_a^{(1)} = j_b^{(1)}, \quad (40a)$$

$$|\phi_{ee}^{(2)}\rangle = |\Phi_C\rangle, \quad \varphi_a^{(2)} = \varphi_b^{(2)} = \frac{\pi}{2}. \quad (40b)$$

This is the driving-free scheme with the highest overall success rate (equal to 1/2) for generating $d = 3$ maximal entanglement. We could equivalently choose $|\phi_{ee}^{(1)}\rangle = |\Psi^-\rangle$ and postselect $j_a^{(1)} \neq j_b^{(1)}$; further, with ξ tuned to an integer, $|\phi_{ee}^{(1)}\rangle = |\Phi^\pm\rangle$ would also work.

Another question is whether it is possible to deterministically generate Schmidt coefficients $\{\sqrt{2/3}, \sqrt{1/3}\}$ in the first iteration. This would allow a deterministic preparation of the state $|\psi^{(1)}\rangle$ [Eq. (37)] by applying unitary corrections of the quantum state (i.e., local driving of nuclear spins) after the first entanglement transfer. Without going into details, our numerical evaluation shows that this is possible by choosing $|\phi_{ee}^{(1)}\rangle = |\Phi_C\rangle$, choosing suitable $\varphi_a^{(1)} = \varphi_b^{(1)}$ (e.g., 1.7125) and fine-tuning the parameter ξ (to an integer multiple of 1.83543).

C. Other probabilistic schemes and optimization

In this subsection, we return to a simpler setting and explore some further schemes for probabilistic entanglement accumulation. In particular, for the initial state $|\psi^{(0)}\rangle$ we consider the equal superposition state from Eq. (26), and further, we choose the same resource state $|\phi_{ee}\rangle$ in all iterations. The arguments for these choices are a possibly easier implementation, as well as a simple generalizability to the multipartite case as discussed in Sec. V. For $d \neq 2^n$ these restrictions result in less optimal bipartite schemes than the one constructed in the previous subsection. Apart from that, for simplicity and because no benefit has been obtained so far from a different choice, we still consider identical nodes ($\xi_a = \xi_b \equiv \xi$) and apply the same CPHASE angle to both nodes, $\varphi_a^{(\nu)} = \varphi_b^{(\nu)} \equiv \varphi^{(\nu)}$.

While it is possible to construct the schemes in this setting from general conditions, for simplicity we identify them by inspection of the output states together with the numerical evaluation of the entanglement. Due to the projecting character of the effective gate $\mathcal{T}_{j_a j_b}^{(\nu)}$, it is of no advantage to use more

than the minimum number of iterations required for generating $E = E_d$; thus, in this subsection $\nu_{\max} = \lceil E_d \rceil$.

From Eq. (6) and Eq. (22) we know that $\mathcal{T}_{j_a, j_b}^{(\nu)}$ is diagonal, and (in the case $\xi = 0$) the diagonal elements are linear combinations of at most four terms of the form $\exp(im\varphi^{(\nu)}/2)$ with integer m and $|m| < d$. For certain discrete phase sets, the output states take a simpler form than for arbitrary angles; e.g., the scheme (30) consists of power-of-two multiples of π/d . Another universal phase set consists of power-of-two fractions $2\pi/2^n$, differing from the previous case for $d \neq 2^n$. For these angles, the number of different values of E over the set of $4^{\nu_{\max}}$ possible measurement outcome series becomes particularly small.

To see that this phase set is also suitable for the probabilistic generation of maximal entanglement, let us start by considering Bell states as the entanglement source, for simplicity $|\phi_{ee}\rangle = |\Psi^\pm\rangle$, and postselecting $j_a^{(\nu)} = j_b^{(\nu)}$ in each iteration ν . For this choice, the state $|\psi^{(\nu)}\rangle$ has the following coefficients in the computational basis,

$$\langle \psi^{(\nu)} \rangle_{i_a, i_b} = \langle i_a, i_b | \psi^{(\nu)} \rangle = \frac{1}{2^{\nu/2} d} \prod_{\mu=1}^{\nu} \cos\left(\frac{i_a - i_b}{2} \varphi^{(\mu)}\right). \quad (41)$$

Now, we choose the phase set $\{\varphi^{(\nu)}\}$ ($\nu = 1, \dots, \nu_{\max}$) with

$$\varphi^{(\nu)} = \frac{2\pi}{2^\nu} (2p^{(\nu)} + 1), \quad \nu_{\max} = \lceil E_d \rceil, \quad (42)$$

where $p^{(\nu)}$ are arbitrary non-negative integers and are typically chosen as $p^{(\nu)} = 0$. With this choice, we find that the state becomes a two-qudit Bell state, $\psi^{(\nu)} = \mathbb{1}_d/d$ with norm $1/\sqrt{d}$. For $d \neq 2^n$, any other measurement outcome series (i.e., measuring $j_a^{(\nu)} \neq j_b^{(\nu)}$ in one or more iterations) results in a partially entangled state. Thus, the scheme (42) generates $E = E_d$ with success rate $P = 1/d$ for such d , while coinciding with the deterministic scheme (30) for $d = 2^n$.

The top panel of Fig. 4 shows the accumulation of entanglement for $d = 3$ based on the phase set (42) for the state $|\phi_{ee}\rangle = |\Psi^\pm\rangle$, independently of ξ . The non-deterministic entanglement transfer is generally dependent on the choice of $|\phi_{ee}\rangle$, and it is worth exploring other states. For states other than $|\Psi^\pm\rangle$, oscillating modulations appear, typically with period π/ξ . For $|\phi_{ee}\rangle = |\Phi^\pm\rangle$, exact maximal entanglement is reached only for ξ being an integer multiple of $2^{\nu_{\max}-1}$ (i.e., ξ integer and even for $d = 3$), and the success rate is the same as for $|\phi_{ee}\rangle = |\Psi^\pm\rangle$. For $|\phi_{ee}\rangle = |\Phi_C\rangle$, on the other hand, only near-maximal entanglement is reached, but the success rate can be higher as discussed in the following.

We observe that for any $d \geq 2$, the protocol (42) is the only one generating maximal entanglement exactly and with finite probability, and for $d \neq 2^n$ this requires $|\phi_{ee}\rangle$ to be a Bell state. However, if we relax our goal from maximal to near-maximal entanglement, there might be other schemes with a possibly higher success rate. As an example, consider the case $|\phi_{ee}\rangle = |\Phi_C\rangle$ and $d = 3$ with the postselection from above (lowest panel of Fig. 4), for which we numerically find the optimal phase set $(\pi, 0.575\pi)$ with $E/E_d \approx 0.989$ and a success probability $P \approx 0.258$. It turns out that in this particular case

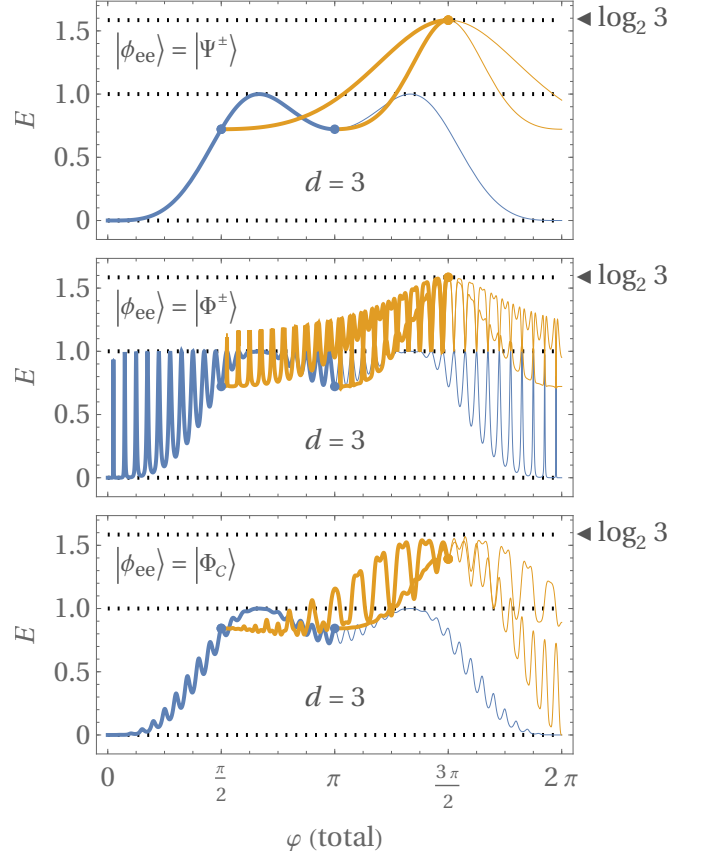


FIG. 4. Generating maximal entanglement in two iterations for $d = 3$, using a postselection of $j_a^{(\nu)} = j_b^{(\nu)}$ in each iteration ν . Different panels correspond to different entangled electron states as indicated. The electron qubit splitting parameter is chosen to be $\xi = 20$.

we can drop the postselection in the first iteration and still obtain exactly the same entanglement $E = E(\varphi^{(1)} = \pi, \varphi^{(2)})$; the phase set above (where the order now matters) then leads to the same $E/E_d \approx 0.989$ with a success probability twice as large, $P \approx 0.516$.

A similar numerical optimization is also possible for higher $d \neq 2^n$, but depends on where the weight is put in the trade-off between entanglement E and success rate P . From an alternative viewpoint, it could also be relevant to optimize the expected entanglement $\langle E \rangle$ averaged over all measurement outcomes. Interestingly, we find that for this purpose, $|\phi_{ee}\rangle = |\Phi_C\rangle$ is the optimal source state (for a properly tuned parameter ξ), and the optimal phase set is essentially just the set (42) (with at most marginal deviations). Before we discuss this sort of optimization in more detail, it is thus worth inspecting the set of entangled states generated by the phase set (42). A statistical evaluation is shown for up to $d = 16$ in Table I. As for the postselected results discussed above, the expected entanglement for this phase set is periodic in ξ with maxima at integer multiples of $2^{\nu_{\max}-1}$; note further that for phase set (42) and such values of ξ , the Bell states $|\Psi^\pm\rangle$ and $|\Psi^\pm\rangle$ are equivalent in terms of the generated entanglement. The grey rows indicate the dimensions $d = 2^n$, for which

the scheme coincides with (30) and hence works deterministically. The worst ratio $\langle E \rangle / E_d$ is typically found for the dimensions directly above each 2^n , with an increase towards the next perfect row, $d = 2^{n+1}$. Comparing Bell and two-qubit cluster states, we find that the latter allows higher $\langle E \rangle$, with a weaker dependence of the entanglement on the measurement outcomes. The cluster state is also the best for optimizing $\langle E \rangle$ by adapting the CPHASE angles as discussed in the remainder.

For completeness, let us first discuss the optimization in the case of Bell states. The upper panel of Fig. 5 shows the expected entanglement for $|\phi_{ee}\rangle = |\Psi^\pm\rangle$, again for $d = 3$ and the phase set (42). The phase set (42) leads to $\langle E \rangle \approx 1.195$; numerical optimization yields $\langle E \rangle \approx 1.224$ for the phase set $\{\varphi^{(\nu)}\} \approx (2.673, 1.617)$, i.e., just a slight improvement. For all other source states, the ξ -dependence of the expected entanglement could generally make the optimization more complicated. The thin dashed lines in Fig. 5 are for the hypothetical case $\xi = 0$. In the case $|\phi_{ee}\rangle = |\Phi^\pm\rangle$ the oscillations may indeed enhance $\langle E \rangle$ over the $\xi = 0$ case, but the optimized $\langle E \rangle$ remains lower than that obtained by $|\phi_{ee}\rangle = |\Phi_C\rangle$, so we do not analyze it further.

For $|\phi_{ee}\rangle = |\Phi_C\rangle$ the case $\xi = 0$ is relevant again, because for most d it constitutes an upper bound for the optimized $\langle E \rangle$, which is also reached by fine tuning the actual parameter $\xi \gg 1$ to an integer multiple of $2^{\nu_{\max}-1}$. We now analyze the question whether $\langle E \rangle$ can be optimized, depending on d . For $d = 2^n$ the scheme (42) is perfect, and obviously no optimization is possible. For any $d = 2^n - 1$, such as $d = 3$ and $d = 7$, we also find that no optimiza-

			$\Phi^\pm\rangle$ or $\Psi^\pm\rangle$			$\Phi_C\rangle$				
d	ν_{\max}	E_d	$\langle E \rangle$	$\frac{\langle E \rangle}{E_d} \%$	#(E)	$\sigma(E)$	$\langle E \rangle$	$\frac{\langle E \rangle}{E_d} \%$	#(E)	$\sigma(E)$
2	1	1	1	100	1	0	1	100	1	0
3	2	1.585	1.195	75.4	2	0.276	1.392	87.8	1	0
4	2	2	2	100	1	0	2	100	1	0
5	3	2.322	1.881	81.0	5	0.354	2.065	88.9	3	0.077
6	3	2.585	2.274	88.0	4	0.237	2.372	91.8	4	0.106
7	3	2.807	2.617	93.2	2	0.078	2.676	95.3	1	0
8	3	3	3	100	1	0	3	100	1	0
9	4	3.170	2.765	87.2	9	0.432	2.934	92.6	10	0.075
10	4	3.322	2.906	87.5	9	0.329	3.055	92.0	12	0.079
11	4	3.459	3.072	88.8	9	0.239	3.205	92.7	10	0.051
12	4	3.585	3.277	91.4	8	0.204	3.377	94.2	10	0.050
13	4	3.700	3.444	93.1	8	0.118	3.516	95.0	9	0.028
14	4	3.807	3.635	95.5	6	0.076	3.672	96.4	8	0.032
15	4	3.907	3.814	97.6	2	0.025	3.832	98.1	1	0
16	4	4	4	100	1	0	4	100	1	0

TABLE I. Entanglement generation with the phase set (42), with Bell or cluster states as a resource. $\langle E \rangle$ is the expected entanglement, #(E) is the number of different E occurring in the set, and $\sigma(E)$ is the standard deviation. The values of $\frac{\langle E \rangle}{E_d}$ are given in %. Decimal numbers are rounded to a fixed number of visible digits. Note that the number of elements (different measurement results) is $2^{2\nu_{\max}}$ in general, or $2^{\nu_{\max}}$ for Bell states by combining equivalent measurement results. The parameter ξ is set to an integer multiple of $2^{\nu_{\max}-1}$ for $|\Phi^\pm\rangle$ and $|\Phi_C\rangle$, or arbitrary for $|\Psi^\pm\rangle$.

tion is possible; further, for this phase set all measurement outcome series lead to the same E , see Table I. For other d we find that just marginal optimization is possible and requires just tiny corrections applied to one or several phases $\varphi^{(\nu)}$ from set (42); these corrections also raise the number of different values E in the outcome set. Furthermore, these corrections also break the above-mentioned periodicity of $\langle E \rangle$ in ξ , so that many parameters affect the optimization procedure; however, it is roughly sufficient to consider the case $\xi = 0$ because the corrections are so tiny that the periodicity still holds approximately, as becomes evident from the following examples. For $d = 5$ and $\xi = 0$, two out of three phases are slightly altered, $\{\varphi^{(\nu)}\} = (\pi, \frac{\pi}{2} + 0.091, \frac{\pi}{4} - 0.033)$, leading to $\langle E \rangle \approx 2.072$, which corresponds to an improvement of $\sim 0.3\%$ over the result 2.065 from Table I. For $d = 5$, but with $\xi = 20$, the same two phases are slightly altered, $\{\varphi^{(\nu)}\} = (\pi, \frac{\pi}{2} + 0.028, \frac{\pi}{4} - 0.008)$, leading to $\langle E \rangle \approx 2.073$, so the difference to $\xi = 0$ is negligible. For $d = 6$ and $\xi = 0$, the optimal phases are $\{\varphi^{(\nu)}\} = (\pi, \frac{\pi}{2} - 0.020, \frac{\pi}{4} - 0.0006)$, leading to an improvement of only $\sim 0.02\%$ over the result $\langle E \rangle \approx 2.372$. Therefore, we conclude at least for up to $d = 8$ that the phase set (42) is exactly equal or very close to the optimal one for maximizing $\langle E \rangle$ without postselection, if we set ξ to any one of the (nearly) optimal values at integer multiples of $2^{\nu_{\max}-1}$.

V. MULTIPARTITE ENTANGLEMENT

The extension of our scheme to more than two nodes works to some extent analogously to the case $d = 2$ described for cluster states in Ref. [17]. This means that genuine multipartite entanglement may be generated by successively establishing entanglement links between each two linked nodes of a cluster, where we denote the number of nodes by M .

As a simple example, consider a row of $M = 3$ nodes labeled $(a), (b), (c)$, the case of pairwise Bell states used as the resource, $|\phi_{ee}\rangle = |\Psi^+\rangle$, and the special case of postselection $j_K^{(\nu)} = j_{K'}^{(\nu)}$ for any ν and the two nodes K, K' being entangled. With nuclear spins initialized in $|+_d\rangle$, a two-qudit Bell state on nodes (a) and (b) can be generated with $P = 1/d$ for any d using phase set (42), i.e., by the operation

$$\mathcal{Q}^{(a,b)} = \prod_{\nu=1}^{[E_d]} \mathcal{T}_{j_a^{(\nu)}=j_b^{(\nu)}}(|\Psi^+\rangle, 2\pi/2^\nu). \quad (43)$$

Then the successive application of this scheme to pairs (a, b) and (b, c) corresponds to

$$\left(\mathbb{1}_d^{(a)} \otimes \mathcal{Q}^{(b,c)} \right) \cdot \left(\mathcal{Q}^{(a,b)} \otimes \mathbb{1}_d^{(c)} \right) \quad (44)$$

and results in a tripartite qudit Greenberger-Horne-Zeilinger (GHZ) state, $(1/\sqrt{d}) \sum_{i=0}^{d-1} |i\rangle \otimes |i\rangle \otimes |i\rangle$, with success rate $1/d^2$. We note that since \mathcal{Q} is diagonal, the order of building up entanglement does not matter; for example, we could first generate 1 ebit for each pair (a, b) and (b, c) , and then add further entanglement to both pairs.

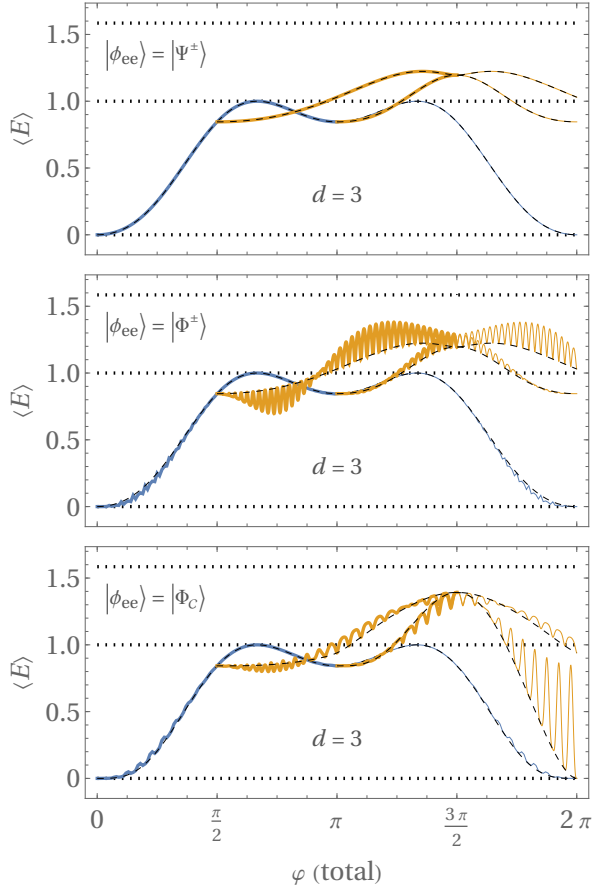


FIG. 5. Expected entanglement without postselection for $d = 3$, for three different types of electron resource states. The electron qubit splitting parameter is chosen to be $\xi = 20$ for the solid lines, while the black thin dashed lines are for $\xi = 0$.

The same principle can be applied to longer chains of modules (higher M), if each two neighbouring sites can be addressed with this scheme. The special case ($|\Psi^+\rangle$, $j_K^{(\nu)} = j_{K'}^{(\nu)}$) above then results in an M -partite qudit GHZ state, which could find application in several quantum networking proposals in QC.

For $d = 2^n$ qudits, the non-postselected outcomes ($j_K^{(\nu)} \neq j_{K'}^{(\nu)}$ for some ν, K, K') for $M = 2$ also result in a maximally entangled state, see Sec. IV A. Thus, a natural question, but beyond the scope of this paper, is whether the unselected multipartite states ($M > 2$) for $d = 2^n$ belong to the same entanglement class as the qudit GHZ state.

VI. DISCUSSION

The nuclear spin quantum memory and transfer scheme presented here may be understood as a higher-dimensional version of the qubit scheme for ^{15}NV centers [17, 34]. For brevity we have not discussed some technical details of the node-node entangling mechanism, which are essentially independent of the nuclear spin providing the memory qudit.

An example is the spin-echo technique required to disentangle electron and nuclear spins in each node upon an unsuccessful entangling attempt by the single-photon interference scheme.

Based on the analogy with these works, we may adopt the benchmark analysis [17] by adjusting parameters accordingly. The ^{14}NV center with $I = 1$ has comparable parameter values and from this aspect should achieve similar fidelities as the ^{15}NV center. However, in this case ($d = 3$) a slower generation of entanglement links is to be expected because one requires either a repeat-until-success entanglement transfer or intermittent driving operations as derived in Sec. IV B.

On the other hand, defect centers with truly high nuclear spins have remarkable properties which make them substantially more suitable for building a fault-tolerant architecture. In comparison with ^{14}NV or ^{15}NV , their Ising hyperfine components are an order of magnitude larger and their nuclear spin coherence times are typically much longer. Due to the first property, the driving-free deterministic transfer scheme itself from Sec. IV A is expected to take at most a few μs . The fact that nuclear spin driving might be required for initialization and final state corrections becomes less problematic owing to the second property.

Another feature adopted from Ref. [17] is the modular structure of the approach, which makes it suitable for the creation of larger clusters. We explicitly confirm that genuine multipartite entanglement may be generated successively by applying the scheme to each two neighbouring network nodes. Apparently, the higher d , the more rapid is the scaling of the entanglement with the number of parties. For the particular application of our scheme in MBQC, the possibility of preparing dedicated states such as higher-dimensional cluster states remains to be investigated.

VII. SUMMARY

We have analyzed methods to accumulate entanglement in nuclear spin memory qudits by repeated entanglement transfer from their respective electron spin communication qubit, mediated by the native Ising coupling. Based on a universal model, our study is applicable to a wide range of platforms, such as the ^{51}V defect center in silicon carbide and the ^{73}Ge center in diamond. The protocol that we consider to have the highest practical relevance is described by a universal phase set, Eq. (30), and generates maximal entanglement deterministically for $d = 2^n$ qudits. The application of our scheme to larger quantum networks opens the possibility of realizing higher-dimensional qudit versions of several QC protocols. We have also pointed out some crucial properties of entanglement transfer which could be of importance even in the case $d = 2$.

ACKNOWLEDGEMENTS

We acknowledge funding from the German Federal Ministry of Education and Research (BMBF) under Grant Agreement No. 13N16212 (SPINNING), and the European Union

under grant agreement No. 101186889 (QuSPARC).

Appendix A: Conditions for deterministic generation of maximal entanglement

Here we evaluate a necessary and sufficient condition for generating d -ranked maximal entanglement in some iteration ν (the final one if successful) of entanglement transfer. If $|\psi_{j_a j_b}^{(\nu)}\rangle$ is rank- d maximally entangled, this means that the matrix $(d/P_{j_a j_b}^{(\nu)})^{1/2}\tilde{\psi}_{j_a j_b}^{(\nu)}$ is unitary. The coefficient matrix $\tilde{\psi}_{j_a j_b}^{(\nu)}$ is given for a general two-qubit resource state $|\phi_{ee}\rangle$ in Eq. (13). Evaluating the equation $\tilde{\psi}_{j_a j_b}^{(\nu)}(\tilde{\psi}_{j_a j_b}^{(\nu)})^\dagger = (P_{j_a j_b}^{(\nu)}/d)\mathbb{1}_d$, we obtain the following condition ,

$$\begin{aligned} \Lambda_{K,00} - (-1)^{j_a} \Lambda_{K,10} - (-1)^{j_b} \Lambda_{K,01} + (-1)^{j_a+j_b} \Lambda_{K,11} \\ = \frac{4}{d} P_{j_a j_b}^{(\nu)} \mathbb{1}_d, \end{aligned} \quad (\text{A1})$$

for $K = a$, where the matrices are defined as

$$\Lambda_{a,00} \equiv (c_{00}^2 + c_{01}^2)S_\downarrow + (c_{10}^2 + c_{11}^2)\mathcal{U}_a S_\downarrow \mathcal{U}_a^\dagger, \quad (\text{A2a})$$

$$\Lambda_{a,10} \equiv (c_{00}c_{10} + c_{01}c_{11})S_\downarrow \mathcal{U}_a^\dagger + \text{h.c.}, \quad (\text{A2b})$$

$$\begin{aligned} \Lambda_{a,01} \equiv c_{00}c_{01}\sqrt{S_\downarrow}\mathcal{U}_b^* \sqrt{S_\downarrow} + c_{10}c_{11}\mathcal{U}_a \sqrt{S_\downarrow}\mathcal{U}_b^* \sqrt{S_\downarrow}\mathcal{U}_a^\dagger \\ + \text{h.c.}, \end{aligned} \quad (\text{A2c})$$

$$\begin{aligned} \Lambda_{a,11} \equiv c_{00}c_{11}\sqrt{S_\downarrow}\mathcal{U}_b^* \sqrt{S_\downarrow}\mathcal{U}_a^\dagger + c_{01}c_{10}\sqrt{S_\downarrow}\mathcal{U}_b^\dagger \sqrt{S_\downarrow}\mathcal{U}_a^\dagger \\ + \text{h.c..} \end{aligned} \quad (\text{A2d})$$

Without loss of generality we have taken the coefficients $c_{j_a j_b}$ of the two-qubit state, Eq. (2), to be real. We do not make any assumption about its entanglement E_{ee} . Similarly, from $(\tilde{\psi}_{j_a j_b}^{(\nu)})^\dagger \tilde{\psi}_{j_a j_b}^{(\nu)} = (P_{j_a j_b}^{(\nu)}/d)\mathbb{1}_d$ we obtain Eq. (A1) for $K = b$, where the matrices $\Lambda_{b,jj'}$ for node b are obtained from the matrices $\Lambda_{a,jj'}$ by swapping nodes ($a \leftrightarrow b$) and coefficient indices ($c_{jj'} \leftrightarrow c_{j'j}$).

We investigate the condition for deterministic entanglement generation, in which case Eq. (A1) needs to hold for all four combinations of (j_a, j_b) . This allows us to solve the four equations for the four matrices (each for $K = a, b$) to obtain that each one is the identity matrix multiplied with a scalar, namely,

$$\Lambda_{K,00} = \frac{1}{d}\mathbb{1}_d, \quad (\text{A3a})$$

$$\Lambda_{K,10} = -\frac{2}{d} \left(P_{00}^{(\nu)} + P_{01}^{(\nu)} - P_{10}^{(\nu)} - P_{11}^{(\nu)} \right) \mathbb{1}_d, \quad (\text{A3b})$$

$$\Lambda_{K,01} = \frac{2}{d} \left(P_{01}^{(\nu)} - P_{10}^{(\nu)} \right) \mathbb{1}_d, \quad (\text{A3c})$$

$$\Lambda_{K,11} = \frac{2}{d} \left(P_{00}^{(\nu)} + P_{11}^{(\nu)} - \frac{1}{2} \right) \mathbb{1}_d. \quad (\text{A3d})$$

We start by inspecting the first equation, (A3a). Defining $c_{00}^2 + c_{01}^2 = 1 - c_{10}^2 + c_{11}^2 \equiv \tau_a/2$ and $c_{00}^2 + c_{10}^2 = 1 - c_{01}^2 + c_{11}^2 \equiv \tau_b/2$ (with $0 \leq \tau_K \leq 2$) we can express it as

$$\mathcal{U}_K^\dagger \tau_K S_\downarrow \mathcal{U}_K = \frac{2}{d} \mathbb{1}_d - (2 - \tau_K) S_\downarrow. \quad (\text{A4})$$

This equation puts constraints on the Schmidt coefficients delivered by the previous iteration $\nu - 1$. Since \mathcal{U}_K is unitary, the entries on the diagonal of $\tau_K S_\downarrow$ must be, up to reordering, the same as those on the r.h.s. of the equation. However, the diagonal entries on the r.h.s. are reversely ordered in comparison with that of $\tau_K S_\downarrow$, and it follows that $\tau_K S_\downarrow + (2 - \tau_K) S_\uparrow = (2/d)\mathbb{1}_d$, where S_\uparrow is obtained from S_\downarrow by reversing the order of diagonal elements. Thus, the diagonal entries of S_\downarrow (and S_\uparrow) come in pairs $\{1/d + (2 - \tau_K)\varepsilon_i, 1/d - \tau_K\varepsilon_i\}$ (with $0 \leq \varepsilon_i$ for $i = 1, \dots, \lfloor d/2 \rfloor$, and one further unpaired central element $1/d$ in the case of odd d). Now, since the diagonal elements are squared Schmidt coefficients or zeros, they must sum up to 1, which yields $\tau_a = \tau_b = 1$. Therefore, the paired diagonal elements of S_\downarrow are $1/d \pm \varepsilon_i$ with $0 \leq \varepsilon_i \leq 1/d$, for $i = 1, \dots, \lfloor d/2 \rfloor$, and one further unpaired central element $1/d$ in the case of odd d . (This is not a constraint for $d = 2$.) Note that these constraints imply that it is impossible to deterministically generate maximal entanglement for odd d when the previous state is even-ranked with equal Schmidt coefficients (so that the strategy derived here does not combine with the strategy from Sec. II B 1 to give a complete strategy for odd d). The condition (A4) can now be restated as

$$\mathcal{U}_K^\dagger S_\downarrow \mathcal{U}_K = \frac{2}{d} \mathbb{1}_d - S_\downarrow = S_\uparrow \quad (\text{A5})$$

In the following, the term block refers to a ‘degenerate’ subspace in which diagonal elements of S_\downarrow (or S_\uparrow) are identical. We take $E^{(\nu-1)} < E_d$ as we want to increase the qudit entanglement, so there is at least one non-vanishing ε_i and hence there are at least two blocks. Eq. (A5) implies that the matrices \mathcal{U}_K must be block-antidiagonal, each block being unitary. The swapped version of this equation, $\mathcal{U}_K^\dagger S_\uparrow \mathcal{U}_K = S_\downarrow$, must also hold since blocks are arranged symmetrically with respect to the center.

Another constraint derives on the entanglement resource state $|\phi_{ee}\rangle$. Since $\tau_a = \tau_b = 1$, it must have the form

$$\phi_{ee} = \begin{pmatrix} \sigma_{00}c & \sigma_{01}\sqrt{1/2 - c^2} \\ \sigma_{10}\sqrt{1/2 - c^2} & \sigma_{11}c \end{pmatrix} \quad (\text{A6})$$

with $0 \leq c \leq 1/\sqrt{2}$ and arbitrary sign factors $\sigma_{j_a j_b}$. Let us define $\kappa_\sigma \equiv (\sigma_{00}\sigma_{11} + \sigma_{01}\sigma_{10})/2 \in \{-1, 0, 1\}$ and $\kappa_c \equiv c\sqrt{1/2 - c^2}$. An EPR pair (any maximally entangled two-qubit state, taking coefficients real) is of the form (A6) as its matrix $\sqrt{2}\phi_{ee}$ is unitary, and is characterized by $\kappa_\sigma\kappa_c = 0$; in particular $\kappa_c = 0$ corresponds to a Bell state and $\kappa_\sigma = 0$ together with $\kappa_c = 1/4$ to a two-qubit cluster state.

Eqs. (A3b)-(A3d) can now be written as

$$-\sigma_{10}\sigma_{11}\kappa_\sigma\kappa_c(\mathcal{U}_K S_\downarrow + \text{h.c.}) = \frac{2}{d} \left(P_{00}^{(\nu)} + P_{01}^{(\nu)} - P_{10}^{(\nu)} - P_{11}^{(\nu)} \right) \mathbb{1}_d, \quad (\text{A7a})$$

$$\sigma_{00}\sigma_{01}\kappa_c\sqrt{S_\downarrow}\mathcal{U}_b^*\sqrt{S_\downarrow} + \sigma_{10}\sigma_{11}\kappa_c\mathcal{U}_a\sqrt{S_\downarrow}\mathcal{U}_b^*\sqrt{S_\downarrow}\mathcal{U}_a^\dagger + \text{h.c.} = \frac{2}{d} \left(P_{01}^{(\nu)} - P_{10}^{(\nu)} \right) \mathbb{1}_d, \quad (\text{A7b})$$

$$\sigma_{00}\sigma_{11}c^2\sqrt{S_\downarrow}\mathcal{U}_b^*\sqrt{S_\downarrow}\mathcal{U}_a^\dagger + \sigma_{01}\sigma_{10}(\frac{1}{2} - c^2)\sqrt{S_\downarrow}\mathcal{U}_b^\top\sqrt{S_\downarrow}\mathcal{U}_a^\dagger + \text{h.c.} = \frac{2}{d} \left(P_{00}^{(\nu)} + P_{11}^{(\nu)} - \frac{1}{2} \right) \mathbb{1}_d. \quad (\text{A7c})$$

These equations must also hold when swapping $a \leftrightarrow b$ and $\sigma_{01} \leftrightarrow \sigma_{10}$. The S -matrices may be commuted to the left using the generalized commutation relation (A5) along with its swapped version ($S_\downarrow \leftrightarrow S_\uparrow$). On the l.h.s. of Eqs. (A7a),(A7b), each term contains a product of an odd number of \mathcal{U}_K -matrices and is thus block-antidiagonal (in particular, since there are at least two blocks, the upper left element of the matrix is zero), while the r.h.s. is diagonal, hence both sides must vanish. From both r.h.s. we obtain that $P_{00}^{(\nu)} = P_{11}^{(\nu)} \equiv P_{\text{eq}}^{(\nu)}$ and $P_{01}^{(\nu)} = P_{10}^{(\nu)} = (1 - P_{\text{eq}}^{(\nu)})/2$. Note that this is not a separate constraint, i.e., it is fulfilled for any state $|\psi^{(\nu-1)}\rangle$ and conditional operations \mathcal{U}_K . Setting the l.h.s. of Eq. (A7a) equal to zero, we obtain that either $|\phi_{ee}\rangle$ is an EPR pair ($\kappa_\sigma\kappa_c = 0$), or $\mathcal{U}_K S_\downarrow + \mathcal{U}_K^\dagger S_\uparrow = 0$. There is no unitary \mathcal{U}_K that fulfills the latter equation unless all ε_i vanish, which we have excluded. Hence, $|\phi_{ee}\rangle$ must be an EPR pair. This is trivial in the case $E^{(\nu-1)} = E^{(\nu)} - 1$ (with $E^{(\nu)} = E_d$), but not for higher $E^{(\nu-1)}$. We are now left with

$$\kappa_c\sqrt{S_\downarrow S_\uparrow} \left[\mathcal{U}_a, \left(\mathcal{U}_b + \mathcal{U}_b^\dagger \right)^\top \right] = 0, \quad (\text{A8a})$$

$$\sqrt{S_\downarrow S_\uparrow} \left[c^2 \mathcal{U}_a \mathcal{U}_b^\top - (\frac{1}{2} - c^2) \mathcal{U}_a \mathcal{U}_b^* + \text{h.c.} \right] = \bar{\sigma}_c \frac{2P_{\text{eq}}^{(\nu)} - 1}{d} \mathbb{1}_d, \quad (\text{A8b})$$

where $\bar{\sigma}_c \equiv \sigma_{00}\sigma_{11}$ for $c \neq 0$, and $\bar{\sigma}_c \equiv -\sigma_{01}\sigma_{10}$ for $c = 0$ ($|\phi_{ee}\rangle = |\Psi^\pm\rangle$); we have used that $\sigma_{00}\sigma_{01}\sigma_{10}\sigma_{11} = -1$, which follows from $\kappa_\sigma = 0$ or can be freely chosen in the case $\kappa_c = 0$. Eqs. (A8) must also hold when replacing $a \leftrightarrow b$.

In the case $E^{(\nu-1)} = E^{(\nu)} - 1$, the goal considered here is equivalent with that from Sec. II B 1, with $E_{ee} = 1$. Indeed, under the constraints derived from Eq. (A4), this case requires that d is even and $|\psi^{(\nu-1)}\rangle$ is $r^{(\nu-1)} = d/2$ -ranked maximally entangled, hence $\varepsilon_i = 1/d$ for all i , and the matrix $S_\downarrow S_\uparrow$ is zero, so that Eqs. (A8) are fulfilled and the constraint (A5) reduces to Eq. (15).

The other case is $E^{(\nu-1)} > E^{(\nu)} - 1$, which means that $r^{(\nu-1)} > d/2$ and the available target Hilbert space for entanglement transfer is too small to fit the entanglement of the EPR pair. We can further distinguish the case $r^{(\nu-1)} < d$, in which the outermost diagonal blocks of $S_\downarrow S_\uparrow$ are zero and hence, from Eq. (A8b) we obtain $P_{\text{eq}}^{(\nu)} = 1/2$, and the case $r^{(\nu-1)} = d$, in which $S_\downarrow S_\uparrow$ is invertible. In both cases, Eqs. (A8) can be further processed by inspecting diagonal blocks individually. We refer to the antidiagonal blocks of \mathcal{U}_a (\mathcal{U}_b) as $\{\mathcal{A}_\varepsilon\}$ ($\{\mathcal{B}_\varepsilon\}$). Here, $\bar{\varepsilon} = +\varepsilon$ for the blocks in the upper right quarter, $\bar{\varepsilon} = -\varepsilon$ for the ones in the lower

left, and $\bar{\varepsilon} = 0$ for the central block (if existent). Note that the central block must exist for odd d . For outermost blocks in the case $r^{(\nu-1)} < d$ (i.e., blocks with $\pm\varepsilon = \pm 1/d$) no constraint (except unitarity) is obtained. For other blocks (in both cases) we define $\zeta_\varepsilon^{(\nu)} \equiv \bar{\sigma}_c(P_{\text{eq}}^{(\nu)} - 1/2)/\sqrt{1 - d^2\varepsilon^2}$. It is possible to simplify the constraints given in Eqs. (A8) by specifying the resource state $|\phi_{ee}\rangle$. For $c = 1/\sqrt{2}$ (Bell state, $|\phi_{ee}\rangle = |\Phi^\pm\rangle$) we obtain that the real part of the eigenvalues of the matrices $\mathcal{A}_\varepsilon \mathcal{B}_\varepsilon^\top$ must be $\zeta_\varepsilon^{(\nu)}$; this means zero in the case $r^{(\nu-1)} < d$. For $c = 0$ (Bell state, $|\phi_{ee}\rangle = |\Psi^\pm\rangle$) we obtain the same eigenvalue constraint but for the matrices $\mathcal{A}_\varepsilon \mathcal{B}_{-\bar{\varepsilon}}^\top$. For $\kappa_c \neq 0$ (other states $|\phi_{ee}\rangle$) the constraints do not simplify that much. One further special case is $c = 1/2$ (two-qubit cluster state, $|\phi_{ee}\rangle = |\Phi_C\rangle$), for which we obtain that (still for $|\bar{\varepsilon}| < 1/d$ only) the real part of the eigenvalues of the matrices $\mathcal{A}_\varepsilon (\mathcal{B}_\varepsilon - \mathcal{B}_{-\bar{\varepsilon}}^\dagger)^\top$ must be $2\zeta_\varepsilon^{(\nu)}$, as well as the condition

$$\mathcal{A}_\varepsilon (\mathcal{B}_\varepsilon + \mathcal{B}_{-\bar{\varepsilon}}^\dagger)^\top - (\mathcal{B}_{-\bar{\varepsilon}} + \mathcal{B}_\varepsilon^\dagger)^\top \mathcal{A}_{-\bar{\varepsilon}} = 0. \quad (\text{A9})$$

Again, the given conditions for each case are necessary and sufficient for generating d -ranked maximal entanglement starting from $E^{(\nu-1)} > E^{(\nu)} - 1$.

Appendix B: Defect center models

In this Section we derive effective Hamiltonians for two defect centers: the GeV center in diamond and the vanadium defect in silicon carbide.

1. Germanium vacancy center in diamond

The GeV is a split vacancy with an orbital degree of freedom. Following Ref. [15], we derive a low-energy effective Hamiltonian. The magnetic field B is assumed to be aligned along the z -axis. The isolated electron Hamiltonian in the basis $\{|e_+, \uparrow\rangle, |e_-, \downarrow\rangle, |e_-, \uparrow\rangle, |e_+, \downarrow\rangle\}$ is

$$H_e = \frac{1}{2} \begin{pmatrix} \lambda + \gamma_e B & 0 & 2\epsilon & 0 \\ 0 & \lambda - \gamma_e B & 0 & 2\epsilon^* \\ 2\epsilon^* & 0 & -\lambda + \gamma_e B & 0 \\ 0 & 2\epsilon & 0 & -\lambda - \gamma_e B \end{pmatrix} \quad (\text{B1})$$

where λ is spin-orbit coupling and $\epsilon = \alpha - i\beta$ is a strain parameter. The orbital Zeeman effect is neglected as it

is quenched. The hyperfine Hamiltonian H_{hf} is given by Eq. (20), with $I = 9/2$ for ${}^{73}\text{Ge}$. The isolated nuclear spin Hamiltonian H_n , see Eq. (19), is not required for the reasons outlined in Sec. III A.

For $\gamma_e B, |\epsilon| \ll \lambda$ there are two blocks $\{|e_+, \uparrow\rangle, |e_-, \downarrow\rangle\}$ and $\{|e_-, \uparrow\rangle, |e_+, \downarrow\rangle\}$, which are energetically far separate from each other. The two blocks are coupled by the strain ϵ and the perpendicular hyperfine component A_{\perp} . Treating the coupling by a Schrieffer-Wolff transformation, we obtain an effective Hamiltonian $H^{\text{eff}} = H_e^{\text{eff}} + H_{\text{hf}}^{\text{eff}}$ for the lower energy block

$$H_e^{\text{eff}} = -\frac{\lambda}{2} + \gamma_e B S_z - 4|\epsilon|^2, \quad (\text{B2})$$

$$H_{\text{hf}}^{\text{eff}} = A_{\parallel} S_z \otimes I_z - \frac{1}{\lambda} \begin{pmatrix} 0 & \epsilon^* A_{\perp} I_+ \\ \epsilon A_{\perp} I_- & 0 \end{pmatrix}. \quad (\text{B3})$$

Removing the constant (spin-independent) terms, we can write

$$H^{\text{eff}} = \gamma_e B S_z + \text{SAI}, \quad (\text{B4})$$

with the hyperfine tensor

$$\mathbf{A} = \begin{pmatrix} -\alpha A_{\perp}/\lambda & -\beta A_{\perp}/\lambda & 0 \\ \beta A_{\perp}/\lambda & -\alpha A_{\perp}/\lambda & 0 \\ 0 & 0 & A_{\parallel} \end{pmatrix}. \quad (\text{B5})$$

To remove the perpendicular hyperfine component, we consider the parameter regime $(|\epsilon| A_{\perp}/\lambda)^2 \ll |\gamma_e B A_{\parallel}|$, which seems realistic. This allows us to perform another Schrieffer-Wolff transformation. In zeroth order, we are left with the Hamiltonian,

$$H^{\text{eff}} = \gamma_e B S_z + A_{\parallel} S_z I_z. \quad (\text{B6})$$

For vanishing strain $|\epsilon|$ this result is exact, while otherwise, higher-order corrections appear. These corrections have only a marginal influence on the generated entanglement, which can be seen from an evaluation analogous to that in App. C for the NV-type center.

The Hamiltonian (B6) is of the desired form, i.e., it is consistent with the model from Sec. III A. The Zeeman term may be removed by transforming to a rotating frame and the term $A_{\parallel} S_z I_z$ allows us to implement a CPHASE-like gate.

2. Vanadium defect in silicon carbide

Another qudit memory is provided by the V defect in SiC, with nuclear spin $I = 7/2$ for the isotope ${}^{51}\text{V}$ [39, 40]. The level structure of the Kramers doublets formed by the combination of the crystal field, spin-orbit coupling, and strain has been studied in detail in Ref. [41]. The resulting effective Hamiltonian $H^{\text{eff}} = H_e^{\text{eff}} + H_{\text{hf}}^{\text{eff}}$ is, in this case,

$$H_e^{\text{eff}} = \gamma_e B S_z, \quad (\text{B7})$$

$$H_{\text{hf}}^{\text{eff}} = \text{SAI}, \quad (\text{B8})$$

where an irrelevant additive constant in (B7) was omitted, and where the hyperfine tensor \mathbf{A} , assuming strain in x direction, is given by Eq. (23) of Ref. [41],

$$\mathbf{A} = \begin{pmatrix} a^{xx} + a^{xy} & 0 & a^{xz} \\ 0 & a^{xx} - a^{xy} & 0 \\ -a^{zx} & 0 & a^{zz} \end{pmatrix}. \quad (\text{B9})$$

For the ground-state doublet $|1, -, \sigma\rangle$, one finds for the matrix elements $a^{ij} = a_{1,-}^{ij}$ the following expressions, $a^{zz} = a_{11}^z - 2a_{11}^z \cos(\theta_1)$, $a^{xx} = a_{11}^x \sin(\theta_1)$, $a^{xy} = -a_{11}^x [1 + \cos(\theta_1)]$, $a^{xz} = a_{11}^x [1 - \cos(\theta_1)]$, and $a^{xx} = -a_{11}^z \sin(\theta_1)$ [41]. In the case of strain in the x direction, the strain mixing angle is given by $\tan(\theta_1) = 2\epsilon_{11}^x/\lambda_{11}^z$ where $\epsilon_{11}^x = s_{11}^x \epsilon_{xz} + s_{11}^x (\epsilon_{yy} - \epsilon_{xx})/2$ denotes the reduced component of the strain tensor and $\lambda_{11}^z = 529$ GHz the relevant spin-orbit coupling constant. Here, ϵ_{ij} are the strain tensor matrix elements and $s_{11} = 251$ THz and $s'_{11} = 230$ THz are strain-orbital coupling coefficients.

For small strain, $\theta_1/\pi \lesssim 0.1$, and magnetic fields $B \gg 10$ mT, we are in the regime $\gamma_e B \gg a^{xx}, a^{xy}, a^{zz} \gg a^{xz}, a^{zx}$. In this case, the effective Hamiltonian has the same form as for the Ge vacancy center, i.e., Eq. (B6), with the parallel hyperfine coupling $A_{\parallel} \approx a^{zz}$. For unstrained SiC, $a^{zz} = 232$ MHz, while in strained SiC, the coupling decreases monotonically to $a^{zz} = 201$ MHz for $\theta_1 = \pi/2$ [41].

Appendix C: Effect of exchange coupling on nuclear-spin entanglement

We perform a perturbation theory with respect to the perpendicular hyperfine component A_{\perp} , the effect of which is suppressed by the much larger splitting of the electron spin qubit levels. For definiteness, we consider the NV center Hamiltonian (17) from Sec. III A. The isolated nuclear spin part H_n does not play a role for the following perturbation theory and will be omitted. Thus, $H = H_e + H_{\text{hf}}$, with the contributions given in Eqs. (18) and (20). We split the Hamiltonian into the unperturbed part H_0 , which is secular and thus block-diagonal (here, even diagonal),

$$H_0 = D S_z^2 + \gamma_e B S_z + A_{\parallel} S_z I_z, \quad (\text{C1})$$

and the block-offdiagonal perturbation

$$V = \frac{A_{\perp}}{2} (S_- I_+ + S_+ I_-), \quad (\text{C2})$$

which induces virtual transitions between m_s sublevels. The zeroth-order energy of the electron spin is $\epsilon_{m_s} = D m_s^2 + \gamma_e B m_s$. In second-order perturbation theory [42], we find $H \approx H_0 + H^{(2)}$, where $H^{(2)}$ is a correction within each m_s subspace,

$$H_{mm'}^{(2)} = \frac{1}{2} \sum_l V_{ml} V_{lm'} \left[\frac{1}{\epsilon_m - \epsilon_l} + \frac{1}{\epsilon_{m'} - \epsilon_l} \right], \quad (\text{C3})$$

where the index l runs only over states that do not belong to the subspace m_s to which m and m' belong.

To give an explicit example of the Hamiltonian resulting from such a Schrieffer-Wolff transformation, we consider $S = 1$ and $I = 1$ (^{14}NV center) and select the states $m_s = 0$ and $m_s = +1$ as the qubit subspace. We also take $\xi_a = \xi_b \equiv \xi$ again. The unperturbed conditional Hamiltonians from Eq. (21) are

$$h_j^{\text{eff}} = (-1)^j \frac{A_{\text{net}}}{2} \text{diag} (1 + \xi, \xi, -1 + \xi), \quad (\text{C4})$$

and the corrections to be added are given by

$$h_0^{\text{eff,corr}} = \text{diag} (0, \zeta_+, \zeta_+), \quad (\text{C5})$$

$$h_1^{\text{eff,corr}} = -\text{diag} (\zeta_+, \zeta_+ + \zeta_-, \zeta_-), \quad (\text{C6})$$

with $\zeta_{\pm} \equiv A_{\perp}^2/A_{\parallel}/(D \pm \gamma_e B)$. Assuming a large zero-field splitting D , we neglect the Zeeman term in the denominator of ζ_{\pm} for simplicity, so we replace ζ_{\pm} by $\zeta \equiv A_{\perp}^2/A_{\parallel}D$. As an example, for the ^{14}NV center, $\zeta \approx -1.2 \cdot 10^{-3}$. For $|\zeta| \ll 1$, the entanglement transferred onto nuclear spin is subject to a small correction of order $\mathcal{O}(\zeta^2)$, as long as our scheme is sufficiently short, i.e., not extending over many ($\mathcal{O}(1/\zeta)$) periods of $2\pi\hbar/A_{\parallel}$. This is obviously the case if we select

the phase $\varphi^{(\nu)}$ for each iteration from within the first period, which minimizes the impact of decoherence.

To evaluate the influence of the perpendicular hyperfine component, we pick two relevant cases, for which our scheme in the case $\zeta = 0$ results in $E = E_d$ without dependence on ξ . First, we consider the conditional entanglement for $d = 3$ and $|\phi_{ee}\rangle = |\Psi^{\pm}\rangle$, obtained by postselection of $j_a^{(\nu)} = j_b^{(\nu)}$ for all ν . For the phases $\varphi^{(1)} = \pi$ and $\varphi^{(2)} = \pi/2$, the relative reduction of E from $E_d = \log_2 3$ is about $8.2\zeta^2$. This corresponds to a tiny value of about $1.1 \cdot 10^{-5}$ for the parameter value of ζ given above for the ^{14}NV center. The actual maximum of E is shifted to slightly different phases $\{\varphi^{(\nu)}\}$, where the shifts are on the order of ζ . However, for the optimal phases, $1 - E/E_d \approx 9.3 \cdot 10^{-6}$, so there is hardly any benefit. Second, we consider the unconditional expected entanglement for $d = 4$, where the set of phases $(\pi, \pi/2)$ achieves two consecutive complete transfers. Here, the relative reduction of E from the ideal value $E_d = 2$ is about $13.8\zeta^2$. These results should be sufficient to estimate the small influence of A_{\perp} . For higher qudit dimensions, corrections remain within the same order of magnitude. In a realistic setup, these errors are presumably negligible compared to other error sources not included in our model.

[1] I. Fernandez de Fuentes, T. Botzem, M. A. I. Johnson, A. Vaartjes, S. Asaad, V. Mourik, F. E. Hudson, K. M. Itoh, B. C. Johnson, A. M. Jakob, J. C. McCallum, D. N. Jamieson, A. S. Dzurak, and A. Morello, Navigating the 16-dimensional hilbert space of a high-spin donor qudit with electric and magnetic fields, *Nature Communications* **15**, 1380 (2024).

[2] J. A. Gross, Designing codes around interactions: The case of a spin, *Phys. Rev. Lett.* **127**, 010504 (2021).

[3] S. Lim, J. Liu, and A. Ardavan, Fault-tolerant qubit encoding using a spin-7/2 qudit, *Phys. Rev. A* **108**, 062403 (2023).

[4] S. Lim and A. Ardavan, Designing quantum error correction codes for practical spin qudit systems, *Phys. Rev. A* **112**, 022418 (2025).

[5] K. Nemoto, M. Trupke, S. J. Devitt, B. Scharfenberger, K. Buczak, J. Schmiedmayer, and W. J. Munro, Photonic quantum networks formed from NV⁻ centers, *Scientific Reports* **6**, 26284 (2016).

[6] H. J. Briegel and R. Raussendorf, Persistent entanglement in arrays of interacting particles, *Phys. Rev. Lett.* **86**, 910 (2001).

[7] R. Raussendorf and H. J. Briegel, A one-way quantum computer, *Phys. Rev. Lett.* **86**, 5188 (2001).

[8] R. Raussendorf, J. Harrington, and K. Goyal, A fault-tolerant one-way quantum computer, *Annals of Physics* **321**, 2242 (2006).

[9] D. L. Zhou, B. Zeng, Z. Xu, and C. P. Sun, Quantum computation based on d-level cluster state, *Phys. Rev. A* **68**, 062303 (2003).

[10] M. S. Tame, M. Paternostro, C. Hadley, S. Bose, and M. S. Kim, Decoherence-based exploration of d -dimensional one-way quantum computation: Information transfer and basic gates, *Phys. Rev. A* **74**, 042330 (2006).

[11] D.-S. Wang, D. T. Stephen, and R. Raussendorf, Qudit quantum computation on matrix product states with global symmetry, *Phys. Rev. A* **95**, 032312 (2017).

[12] C. Reimer, S. Sciara, P. Roztocki, M. Islam, L. Romero Cortés, Y. Zhang, B. Fischer, S. Loranger, R. Kashyap, A. Cino, S. T. Chu, B. E. Little, D. J. Moss, L. Caspani, W. J. Munro, J. Azaña, M. Kues, and R. Morandotti, High-dimensional one-way quantum processing implemented on d-level cluster states, *Nature Physics* **15**, 148 (2019).

[13] P.-J. Stas, Y. Q. Huan, B. Machielse, E. N. Knall, A. Suleymanzade, B. Pingault, M. Sutula, S. W. Ding, C. M. Knaut, D. R. Assumpcao, Y.-C. Wei, M. K. Bhaskar, R. Riedinger, D. D. Stukachev, H. Park, M. Lončar, D. S. Levonian, and M. D. Lukin, Robust multi-qubit quantum network node with integrated error detection, *Science* **378**, 557 (2022).

[14] C. M. Knaut, A. Suleymanzade, Y.-C. Wei, D. R. Assumpcao, P.-J. Stas, Y. Q. Huan, B. Machielse, E. N. Knall, M. Sutula, G. Baranes, N. Sinclair, C. De-Eknamkul, D. S. Levonian, M. K. Bhaskar, H. Park, M. Lončar, and M. D. Lukin, Entanglement of nanophotonic quantum memory nodes in a telecom network, *Nature* **629**, 573 (2024).

[15] C. Adambukulam, B. C. Johnson, A. Morello, and A. Laucht, Hyperfine spectroscopy and fast, all-optical arbitrary state initialization and readout of a single, ten-level ^{73}Ge vacancy nuclear spin qudit in diamond, *Phys. Rev. Lett.* **132**, 060603 (2024).

[16] A. Morello, J. J. Pla, P. Bertet, and D. N. Jamieson, Donor spins in silicon for quantum technologies, *Advanced Quantum Technologies* **3**, 2000005 (2020).

[17] K. Nemoto, M. Trupke, S. J. Devitt, A. M. Stephens, B. Scharfenberger, K. Buczak, T. Noebauer, M. S. Everitt, J. Schmiedmayer, and W. J. Munro, Photonic architecture for scalable quantum information processing in diamond, *Phys. Rev. X* **4**, 031022 (2014).

[18] T. Giordani, L. Innocenti, A. Suprano, E. Polino, M. Paternostro, N. Spagnolo, F. Sciarrino, and A. Ferraro, Entanglement transfer, accumulation and retrieval via quantum-walk-based

qubit-qudit dynamics, *New Journal of Physics* **23**, 023012 (2021).

[19] A. Delgado, L. Roa, J. C. Retamal, and C. Saavedra, Entanglement swapping via quantum state discrimination, *Phys. Rev. A* **71**, 012303 (2005).

[20] Y. Fu, W. Liu, X. Ye, Y. Wang, C. Zhang, C.-K. Duan, X. Rong, and J. Du, Experimental investigation of quantum correlations in a two-qutrit spin system, *Phys. Rev. Lett.* **129**, 100501 (2022).

[21] P. Koller, T. Astner, B. Tissot, G. Burkard, and M. Trupke, *Strain-enabled control of the vanadium qudit in silicon carbide* (2025).

[22] D. P. Franke, F. M. Hrubesch, M. Künzl, H.-W. Becker, K. M. Itoh, M. Stutzmann, F. Hoehne, L. Dreher, and M. S. Brandt, Interaction of strain and nuclear spins in silicon: Quadrupolar effects on ionized donors, *Phys. Rev. Lett.* **115**, 057601 (2015).

[23] S. Asaad, V. Mourik, B. Joecker, M. A. I. Johnson, A. D. Baczewski, H. R. Firgau, M. T. Madzik, V. Schmitt, J. J. Pla, F. E. Hudson, K. M. Itoh, J. C. McCallum, A. S. Dzurak, A. Laucht, and A. Morello, Coherent electrical control of a single high-spin nucleus in silicon, *Nature* **579**, 205 (2020).

[24] X. Yu, B. Wilhelm, D. Holmes, A. Vaartjes, D. Schwienbacher, M. Nurizzo, A. Kringshøj, M. R. van Blankenstein, A. M. Jakob, P. Gupta, F. E. Hudson, K. M. Itoh, R. J. Murray, R. Blume-Kohout, T. D. Ladd, A. S. Dzurak, B. C. Sanders, D. N. Jamieson, and A. Morello, *Creation and manipulation of schrödinger cat states of a nuclear spin qudit in silicon* (2024).

[25] G. W. Morley, M. Warner, A. M. Stoneham, P. T. Greenland, J. van Tol, C. W. M. Kay, and G. Aeppli, The initialization and manipulation of quantum information stored in silicon by bismuth dopants, *Nature Materials* **9**, 725 (2010).

[26] T. Zhong, J. M. Kindem, J. G. Bartholomew, J. Rochman, I. Craicu, V. Verma, S. W. Nam, F. Marsili, M. D. Shaw, A. D. Beyer, and A. Faraon, Optically addressing single rare-earth ions in a nanophotonic cavity, *Phys. Rev. Lett.* **121**, 183603 (2018).

[27] A. M. Dibos, M. Raha, C. M. Phenicie, and J. D. Thompson, Atomic source of single photons in the telecom band, *Phys. Rev. Lett.* **120**, 243601 (2018).

[28] P. Siyushev, K. Xia, R. Reuter, M. Jamali, N. Zhao, N. Yang, C. Duan, N. Kukharchyk, A. D. Wieck, R. Kolesov, and J. Wrachtrup, Coherent properties of single rare-earth spin qubits, *Nature Communications* **5**, 3895 (2014).

[29] I. Nakamura, T. Yoshihiro, H. Inagawa, S. Fujiyoshi, and M. Matsushita, Spectroscopy of single pr3+ ion in laf3 crystal at 1.5 k, *Scientific Reports* **4**, 7364 (2014).

[30] T. Utikal, E. Eichhammer, L. Petersen, A. Renn, S. Götzinger, and V. Sandoghdar, Spectroscopic detection and state preparation of a single praseodymium ion in a crystal, *Nature Communications* **5**, 3627 (2014).

[31] N. Friis, G. Vitagliano, M. Malik, and M. Huber, Entanglement certification from theory to experiment, *Nature Reviews Physics* **1**, 72 (2019).

[32] S. Bose, V. Vedral, and P. L. Knight, Purification via entanglement swapping and conserved entanglement, *Phys. Rev. A* **60**, 194 (1999).

[33] W.-R. Hannes, R. Finsterhoelzl, and G. Burkard, Fidelity of remotely entangled nuclear spin states in photon-connected multiqubit registers, *Phys. Rev. A* **110**, 052436 (2024).

[34] M. S. Everitt, S. Devitt, W. J. Munro, and K. Nemoto, High-fidelity gate operations with the coupled nuclear and electron spins of a nitrogen-vacancy center in diamond, *Phys. Rev. A* **89**, 052317 (2014).

[35] C. Tabares, E. Zohar, and A. González-Tudela, Tunable photon-mediated interactions between spin-1 systems, *Phys. Rev. A* **106**, 033705 (2022).

[36] F. Omlor, B. Tissot, and G. Burkard, Entanglement generation using single-photon pulse reflection in realistic networks, *Phys. Rev. A* **111**, 012612 (2025).

[37] In Ref. [17] the use of a rotating frame without transforming back effectively sets $\xi = 1/2$.

[38] T. Kraft, C. Ritz, N. Brunner, M. Huber, and O. Gühne, Characterizing genuine multilevel entanglement, *Phys. Rev. Lett.* **120**, 060502 (2018).

[39] B. Tissot and G. Burkard, Spin structure and resonant driving of spin- $\frac{1}{2}$ defects in SiC, *Phys. Rev. B* **103**, 064106 (2021).

[40] B. Tissot and G. Burkard, Hyperfine structure of transition metal defects in SiC, *Phys. Rev. B* **104**, 064102 (2021).

[41] B. Tissot, P. Udarhelyi, A. Gali, and G. Burkard, Strain engineering for transition-metal defects in SiC, *Phys. Rev. B* **109**, 054111 (2024).

[42] R. Winkler, *Spin-orbit Coupling Effects in Two-Dimensional Electron and Hole Systems* (Springer-Verlag Berlin Heidelberg, 2003).